universität wien

MASTERARBEIT / MASTER'S THESIS

Titel der Masterarbeit / Title of the Master's Thesis

Extended Infectivity Assay: Amplification and Detection of Retroviral Contaminations on a Lab-on-a-Chip device

verfasst von / submitted by

Michaela Herlinde Purtscher BSc

angestrebter akademischer Grad / in partial fulfilment of the requirements for the degree of

Master of Science (MSc)

Wien, 2021 / Vienna 2021

Degree programme code as it appears on the student record sheet:	UA 066 834
Degree programme as it appears on the student record sheet:	Masterstudium Molekulare Biologie
Supervisor:	Univ.-Prof. Dipl.-Ing. Dr. Peter Ertl (TU Wien)

Acknowledgments

First and foremost, I'd like to thank my parents, Rosmarie Purtscher and Helmut Gruber for always fostering scientific curiosity in me and for their help and encouragement to reach this goal.

Finishing this thesis would not have been possible without the help of great supervisors, a bunch of very good friends and considerate colleges.

With that I want to thank my practical supervisor Univ.-Prof. Dipl.-Ing. Dr. Peter Ertl for the possibility to learn so much about microfluidic and the opportunity to do the practical work in his labs and providing a cheerful and nice working environment which allowed for many fruitful discussions.

My theoretical supervisor Univ.-Prof. Mag. Dr. Peter Lieberzeit provided invaluable help and guidance finishing this thesis and writing our joint publication, as well as insight into the world of MIPs & quartz crystal microbalance systems.

I like to thank Dr. Andrew Bailey for supporting us with regards to viral systems and providing us with the tools to work with.

A great thanks also goes to all my co-workers over the time, for their help, their inspirations and for the good times we had together. I am especially thankful to Dr. Verena Charwat for her deep friendship and for the wide knowledge she shared with me and Dr. Mario Rothbauer, without whom I would not have been able to write up this thesis hadn't he kept pushing me and reached me so much about writing.

A great thanks also goes to my friend Dr. Stefan Lutzmayer, who not only supported me with his friendship when times were hard and made me see things as they are but also was particularly helpful as copyeditor of my thesis.

I am very grateful to my partner Dr. Brian Reichholf, without his calmness, confidence and reassurances it would have been much harder to write this thesis. He is my bastion of calm and happiness. His help goes beyond the scope of this thesis.

I further want to thank also all my colleges at the FH Technikum Wien for never stopping in believing me being able to finish this thesis.

Extended Infectivity Assay: Amplification and Detection of Retroviral Contaminations on a Lab-on-a-Chip device

CONTENTS

1 Abstract

Studying viruses and virus-host interactions is of great interest to scientists and not limited to new vaccine development. Viral structures are widely employed as gene delivery systems and are also used in novel clinical immunotherapy applications. Retroviruses were the first class of viruses used in gene therapy. Due to their unique feature of stable integration into the host cell genome, genes of interest could be integrated alongside the retroviral genome. Thus, enabling stable gene expression which paved the way for potential treatments especially of monogenetic diseases.

Although retroviruses were rendered replication-deficient, naturally occurring recombination events could still lead to replication-competent viruses. Consequently, strict safety guidelines were introduced that include extensive product testing and the establishment of packaging cell lines.

Here I present a microfluidics-based extended infectivity assay that is based on the co-culture of a virus amplification- and a detection cell line to monitor their growth patterns by tracing the according impedance values. Our developed Lab-on-a-Chip device allows the non-invasive and time-resolved monitoring of the cell cultures over the whole assay time as a result of the embedded impedance microsensors in the polydimethylsiloxane (PDMS) based microfluidic system.

The constant virus amplification is achieved by *M. dunni* cells and permit enhanced early onset of cytopathic effects in the downstream PG-4 detection cell line. This resulted in an assay time of about 3 days when used with the xenotropic murine leukemia virus (x-MuLV) retrovirus model at initial virus titres as low as 1.05×10^4 PFU/ml.

2 Zusammenfassung

Die Untersuchung von Viren und Virus-Wirt-Interaktionen ist für Wissenschaftler von großem Interesse und nicht auf die Entwicklung neuer Impfstoffe beschränkt. Virale Strukturen werden weithin als Gentransport Systeme verwendet und finden auch in neuen klinischen Immuntherapien Anwendung. Retroviren waren die erste Klasse von Viren, die in der Gentherapie verwendet wurden. Aufgrund ihres einzigartigen Merkmals, der stabilen Integration in das Genom der Wirtszelle können Gene von Interesse zeitgleich mit dem retroviralen Genom integriert werden. Dies ermöglicht eine stabile Genexpression, die den Weg für potenzielle Behandlungen insbesondere von monogenetischen Erkrankungen ebnet.

Obwohl Retroviren Replikations-defizient gemacht wurden, könnten natürlich vorkommende Rekombinationsereignisse immer noch zu Replikations-kompetenten Viren führen. Folglich wurden strenge Sicherheitsrichtlinien eingeführt, die umfangreiche Produkttests und die Etablierung von Verpackungszelllinien beinhalten. Hier präsentiere ich einen auf Mikrofluidik basierenden erweiterten Test zur Messung der Infektiosität, der auf der Co-Kultur einer Virusamplifikations- und einer Nachweiszelllinie basiert, und deren Wachstumsmuster anhand von Impedanzwerten mitverfolgt wird. Unser entwickeltes Lab-on-a-Chip-System ermöglicht aufgrund der in dem auf Polydimethylsiloxan (PDMS) basierenden mikrofludischen System eingebetteten Impedanz-Mikrosensoren eine nicht-invasive zeitaufgelöste Überwachung der Zellkulturen über die gesamte Testzeit.

Die konstante Virusamplifikation wird durch *M. dunni*-Zellen erreicht und ermöglicht ein verstärktes frühes Einsetzen zytopathischer Effekte in der stromabwärts gelegenen PG-4-Nachweiszelllinie Dies führte zu einer Testzeit von etwa 3 Tagen, wenn es mit dem xenotropen Maus-Leukämievirus (x-MuLV)-Retrovirus-Modell bei anfänglichen Virustitern von nur 1.05×10^4 PFU/ml verwendet wurde.

3 Motivation and Assay Principle

Today, 6,590 species of viruses have been identified by The International Committee on Taxonomy of Viruses (ICTV) which is only a small part of the over 150,000 estimated existing viruses species [1],[2]. This vast variety of viruses have host ranges comprised of animals, plants, bacteria and fungi. Viruses are classified based on the host range, the genome and capsid structure, the presence or absence of an envelope, pathogenicity and importantly their replication strategy. The life cycle of a virus consists of the attachment and entry into the host cell, followed by the uncoating and processing of the viral genetic information. Thereafter, the biosynthesis of viral components takes place by the host cells organelles and the newly formed viruses maturate. The release from the host cells then occurs either by lysis of the cell, budding off the cell membrane or excretion [3]. Such processes can cause cellular alterations as well as cell death and are described as cytocidal effects. Those include morphological changes, alterations of the cell physiology and the cellular biochemistry, genotoxic changes or more general termed biologic effects. Morphological altering events or cytopathic effects (CPE) post infection, commonly include rounding of the cell, formation of syncytia with adjacent cells and the formation of inclusion bodies. CPE therefore are especially suitable for detection of infected cells and diagnostic approaches since most of them can be observed with little cost and effort, often only by the help of a light microscope and simple sample preparation procedure [4].

Expanding our knowledge of the of virus-cell interactions from the first contact, over cellular transforming effects up to the release of new virions is of great interest when studying adverse effects on organisms; besides, the simplicity of some viral system qualifies for the relative ease of their manipulation. The broad spectrum of virus species and the wide range of permissive hosts they bear tremendous potentials for applications in various life science areas. A compelling healthcare application is the usage of attenuated or inactivated viruses as conventional vaccination agent. Since the eradication of the small pox virus in 1902 [5], the advancements made in these areas led to the emerging field of virotherapy. This term summarises the studies and approaches using native and engineered viruses in cancer therapies, viral immunotherapies or their usage as delivery vehicles for genetic material in gene therapy [6],[7].

To overcome multi-drug resistances, phages, which infect bacteria, are investigated as antibacterial agents in humans [8] as well as bacteria-infected plant crops [9]. Moreover, various viruses are used to engineer viral nanoparticles (VNPs) which permit the development of a variety of applications including the generation of new materials, enhancing stem cell differentiation in the field of tissue engineering or the development of novel diagnostic imaging methods [9].

Detection, quantification and monitoring of interactions between viruses and host cells are not limited to the development of novel approaches but are also fundamental in ensuring pharmaceutical product safety. Plaque-based assays are among the most used methods for the direct quantification of infectious virions potentially present in raw materials or cell lines as well as in the determination of the success of viral clearance studies.

The principle of a plaque assay takes advantage of CPEs caused by viral infections in the host cells. In short, the standard assay protocol includes the application of several dilutions of the virus containing reagent onto fully grown cell layers

usually followed by the coverage with a solid or semisolid overlay to hinder the random spread of the virus. Upon infection, the cell undergoes morphological changes which may cause rounding up and even detachment from the growth substrate or directly leads to cell lysis during the process of viral release. The formed virions then spread to adjacent cells and restart their life cycle. Over time, this is followed by the formation of visible plaques in the cell layer. To enhance the contrast between cell layer and plaques, a staining procedure is usually performed at the end of the culture period which can take up to 14 days, depending on the virus which is to be analysed. The plaque count in relation to the dilutions applied is used to calculate the plaque forming unit/ml (PFU/ml). The PFU represents the infective particles within a given sample, which in viral clearance studies is used to determine the effectives of the applied method [10],[11].

Retroviruses are of particular interest in risk assessment concerning the safety of biotechnology products. It has been shown that in the mouse genome consist of up to 10% of endogenous retroviral sequences. While most of them inactive, others are able to alter the host's genome by insertional mutagenesis [12]. Hence, there is a risk of the expression of retroviral-like particles while using mammalian cell lines to produce biopharmaceuticals. Although most of these particles have been found to be non-infective [13], the risk of obtaining replication-competent particles through recombination events remains.

The murine leukaemia virus (MuLV) is one of the best studied retroviruses and – thanks to its simple genome - became the most used model system for the genus of gammaretroviruses. Furthermore, MuLV is recommended in virus clearance studies when performing plaque-based assays [14][15]. The xenotropic murine leukaemia virus (x-MuLV), originally derived from endogenous sequences of inbred mice, is a well-studied retrovirus that was first isolated from the thymus of five and a half month old NFS swiss mice [16]. The virus can be propagated by the *M. dunni* cell line (*mus terricolour*) without adverse effects. However, x-MuLV infection of mink S+L- and the feline S+L- PG-4 cells causes CPEs, detectable by a focus forming assay, which is based on immunofluorescent labelling of antibodies [17],[18]. Similarly, standard plaque assays can be used in PG-4 cells after infection [19] [20].

In this work, an extended infectivity assay was developed which focuses on the measurement of plaques formed PG-4 in a cell layer upon infection with the x-MuLV. This is achieved by monitoring and analysing the morphological changes employing impendence spectroscopy.

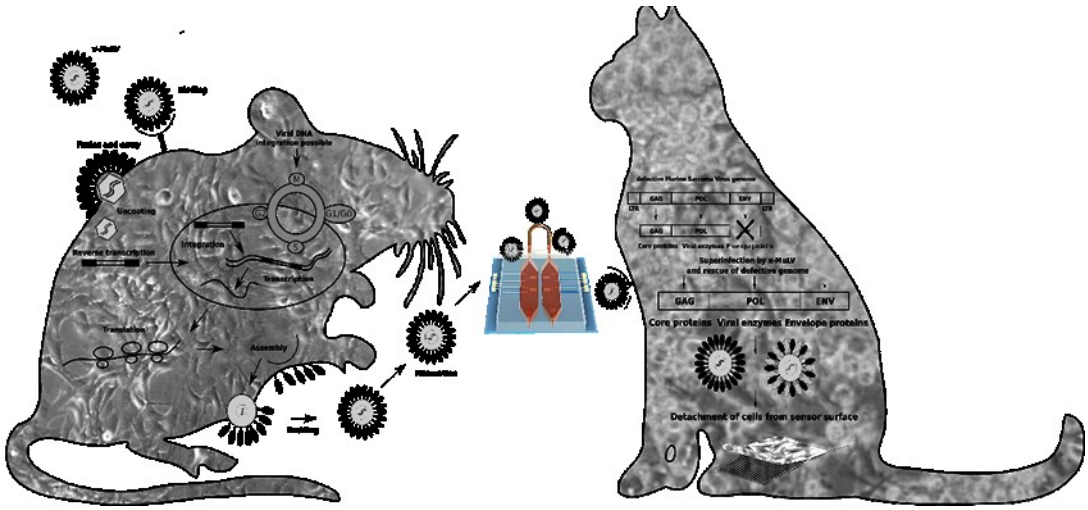

Figure 1: Overview of the assay principle: The left side indicates the life cycle of a retrovirus within *M. dunni* cell. In the middle the device itself with two connected culture chambers (left for *M. dunni* cells and right for PG-4 cells) and the beneath lying impedance sensor array is shown. On the right side the rescue of the defective sarcoma virus through the infection with x-MuLV and the following detachment of PG-4 cells from the sensor surface is illustrated. Adapted from [21]

A two chambered fluidic layer made from polydimethylsiloxane (PDMS) is covalently bound on top of an impedance sensor array. Each sensor consists of 200 fingers with widths and gaps of 5 µm each. The single fluidic chamber provides a cell growth area of 95 mm2, ensuring enough surface for the proliferation of the *M. dunni* virus propagation cell line (left chamber), and the PG-4 detection cell line (right chamber). The top glass seals the chamber and the attachment of the connecting tubing. Upon connection of the two chambers the re-infection rate of the PG-4 cell line is increased through constant provisioning of fresh virus particle by the *M. dunni* cells over the time course of the assay.

The biological basis for this assay, the life cycle of the x-MuLV within the *M. dunni* cells, the rescue of the defective sarcoma genome within the PG-4 cell genome and the following detachment of those cells from the sensor surface are illustrated in Figure 1.

On the left, the simplified life cycle of the retrovirus is indicated. After injecting the virus via an external syringe pump, it binds to the host cell and fuses with the membrane. Subsequently, the virus enters the cytoplasm and the viral RNA genome is set free. The single-stranded viral RNA genome is then reverse transcribed into DNA via its own reverse transcriptase activity. Importantly, the stable integration of the provirus into the host's genome can only occur during the breakdown of the nuclear membrane during the mitosis of the cell. Hence, the x-MuLV can only integrate its genome in actively replicating cells. Following successful integration, the host cellular machinery is exploited to produce new viral proteins that assemble and form mature virions [22]. These are then transported by a constant medium flow of 1.5µl/min to the PG-4 detection cell line.

The sarcoma-positive and leukaemia-negative PG-4 cells harbour a sarcoma genome which is defective in the envelope protein and therefore cannot replicate, indicated on the right in Figure 1. Due to the superinfection with the x-MuLV, which acts as helper virus, the defective sarcoma genome can be rescued [23],[24]. As a consequence, the generation of new virus particles entails the detachment of

PG-4 cells from the surface of the sensor and thus resulting in decreased impedance signal.
Monitoring cellular behaviour by changes in impendence signals is an established technology. It enables tracing of cellular events like the attachment of the cell to the growth substrate, cellular micromotions as a whole as well as indirect monitoring of cell proliferation, due to changes in sensor surface coverage [25][26].
The strengths of the here presented assay lies in the continuous and non-invasive monitoring of both cell lines, and the constant supply of newly formed virions through the propagation cell line and proceeding from the initially applied virus titre. Moreover, it enables short assay times since an onset of viral infection can be detected within 60 to 70 hours after the initial exposure of the culture requiring only low initial virus titre thus reducing the potential risks emerging when working with biohazards. While at the same time samples of unknown or with suspected low virus titre can be analysed without additional upstream processing steps. The establishment of a cell-type specific impedance trace for the propagation cell line enabled a direct performance control of the assay since an unhealthy or dying culture can be identified at any time. Therefore, permitting an early termination and restart of the assay. In addition, the direct measurement of impedance signal omits the need for further staining or fluorescence labelling steps. Although based on standard methods for viral quantification, the presented assay has the potential to not only detect viral presence but also to monitor kinetics between virus and host cell interactions. Furthermore, it is also compatible with downstream quantification with classical polymerase chain reaction (PCR) or molecular imprinted polymers in combination with quartz crystal microbalance measurements.

4 Introduction

4.1 Microfluidic – Technology and Research Field

Originating in 1969, when Lew and Fung published their work on a theoretical model on the blood and air flow in a microcirculatory system [27], the foundation was laid for microfluidic as a technology and research field. In the 1980‘s microfluidics-based technology was first integrated into inkjet printheads and was progressively introduced into the development of DNA chips and micro-electro-mechanical systems (MEMS) [28]. Since then, the field of applications is constantly growing. Microfluidics reflects a highly interdisciplinary field and engages mainly engineers, physicists, chemists, biologists as well as other specialised professionals. It is an enabling technology, especially in life sciences such as pharmacology, biotechnology, ecology as well as medicine. Although already published in 2004, Ducrée & Zengerle gave a comprehensive overview of microfluidics and it massive potential which is still valid today [29].

Microfluidic is the study of fluids, their behaviour and manipulation in a micrometre scale with standard dimensions usually ranging from 10µm to a several 100µm.

Fluid flow itself is characterised by the dimensionless Reynolds number which is defined by Equation 1, whereby fluids with numbers above 2000 slowly progress from a transition state towards states of turbulent flow profiles. Applied on a typical microfluidics platform, the resulting Reynolds numbers are usually below 100. Values lower than 1 dictate a laminar flow profile within such systems.

$$Re = \frac{\rho \, v \, Dh}{\mu}$$

Equation 1: Dimensionless Reynolds number for the characterization of fluids, ρ is the fluid density, ν the main velocity of the fluid, Dh the hydraulic diametre and μ the fluid viscosity.

By engaging the scaling laws, it becomes obvious that at such small dimensions, surface tension, energy dissipation, fluid resistance and diffusion principles become predominant physical parameters; therefore, fluids can be precisely controlled in both spatial and temporal dimensions. Novo P *et al.* give an overview to which extent fluids can be controlled with particular emphasis on the spatial control of cells within microfluidic devices [30].
The utilization of microfluidic systems can lead to a high reduction of overall cost in fields such as genomics, drug discovery and toxicity testing as well as in environmental pollution studies to give some examples [31]. This is not only a result of the high throughput of measurements possible by multiplexing and parallelization of the experiments, therefore increasing accuracy and reproducibility, but foremost due to the reduction in cells, culture reagents and test substances required in these small systems.
Furthermore, for studying cells which naturally experience some sort of shear stress these systems are uniquely suitable to obtain meaningful data by introducing physiological stresses by simply adjusting the fluid flow profiles. One such example are vascular endothelial cells, which build up the inner most layer of blood vessels and are exposed to shear stresses in magnitudes reaching from 1 to 6 dyne/cm^2 in the venous system and up to 10 to 70 dyne/cm^2 in the arterial system [32]. In contrast, the shear stress on cells due to interstitial flow, lies below 1 dyne/cm^2. Because the flow velocity is so low and inhomogeneous, direct and exact measurements have proven to be difficult *in vivo*. However, according to literature the surface shear stress reaches from 0.005 to 0.007 dyne/cm^2 and is peaking around 0.15 dyne/cm^2 [33]. Within a microfluidic system, adjusting this parameter can be easily achieved via external or internal pumps; therefore, better mimicking the physiological environment of *in vitro* cultured cells while maintaining a constant waste removal and nutrient supply.

4.1.1 Micro-electromechanical Systems (MEMS) and Lab-on-Chip (LOC) Devices

In combination with microfluidics, terms such as micro-electromechanical systems (MEMS), lab-on-chip (LOC) and also micro-total-analysis systems (μTAS) are often used synonymously and usually operate in the range of micro- to millimetres. Although they are not used completely interchangeably, they do have similar technology principles in common. While LOC and μTAS technology are more focused on the cellular and analytical components, MEMS as the name

indicates, are more center on the mechanical parts. MEMS is a technology working mostly on a micro- to nanometres scale although whole devices can easily reach a few millimetres. These devices usually contain moveable mechanical parts which are controlled by integrated microelectronic processors. The downsized sensors and actuator, transducing mechanical into electrical signals are often used for measuring temperature, magnetic fields, radiation, pressure and various chemical species [34]. In 1959, the theoretical physicist Richard Feynman introduced the concepts of this technology in a lecture he held at the annual American Physical Society meeting titled "There is plenty room at the Bottom: An Invitation to Enter a New Field of Physics" [35]. Nowadays, MEMS technology is part of inkjet printer heads, cell phones, micro scanners, blood pressure sensors, bio-, and chemo-sensors, to name only a few applications.
As mentioned before, lab-on-chip devices and micro-total-analysis systems are a subset of MEMS technology. For the ease of reading, only the term LOC will be further used in this paper. LOC devices are systems which integrate and automate one or several laboratory tasks including handling steps and analysis techniques usually achieved by integrated valve and pump systems, which are based on microfluidic principles. The potential of LOCs lies in almost all life sciences areas and particularly in point-of-care diagnostics [34]. Despite the described advantages of lab-on-chip devices combined with microfluidics, only a few examples have made it on the market so far. One of those examples is the point-of-care device Triage® (BiositeInc, USA) that is based on the detection of immunofluorescence levels of creatine Kinase in whole blood or plasma samples and can also be used for the diagnosis of myocardial infarction [36]. However, the reasons and challenges of why LOC devices are not yet fully commercialised and available for clinicians as well as private persons is well-described in the review of Mohammend *et al.* [37].

4.1.2 Cell-based Biosensors

One key element of LOC devices are integrated biosensors. In general, a biosensor is an analytical device which converts a biological response into an electrical signal. It consists of a sensitive biological element, a transducer or detector, often with an integrated amplifier and an electronic system for displaying the measured signals. The biological element can be anything from a nucleic acid over enzymes or antibodies to whole cells or even tissue-like structures [38]. With respect to this work, the focus will be on cells and cell layers as the sensitive element. Utilizing cells as the sensitive element within a detection system is of particular interest in the food and biosecurity sectors where they are often used for pathogen and toxin testing [39]. Despite the obvious ethical concerns and the often-questionable translatability of obtained results to human conditions, cell-based systems do have advantages over animal testing. The most obvious ones are cost reduction, the possibility for multiplexed assays and the relatively easy handling and operating such cell- and sensor-based systems compared to the maintenance and execution of animal studies. The simplicity of the cell-based system not only allows for consistent signal recording from 2- and 3-dimensional cultures but also keeps the possibilities of fast modifications of the whole system if proven necessary. Analytes, cell types, cell environments and the biological mechanism addressed can be chosen almost freely, due to the wide variety and technologies

available today. Cellular responses can be investigated on the level of gene expression, protein synthesis and inhibition, cell-signalling pathways, metabolic alterations, apoptotic or necrotic mediated cell death. Additional advantages of small cell-based biosensors are portability and the relative ease of mounting them onto microscopes or similar equipment for real-time monitoring [40]. Based on the transducing principle of biosensor, they can be classified as electrochemical and optical biosensors along with other physical principles such as surface acoustic or calorimetric types [41],[42].

4.1.2.1 Electrical Impedance Spectroscopy for Cell-based Analysis

State-of-the-art *in vitro* analysis techniques are often based on gene and protein profiling as well as immunohistochemistry. These enabled a profound understanding of cellular processes; however, a lot of these techniques are designed as end-point measurements and thus define the termination point of the experiment. Hence, to investigate cellular changes in a time-resolved manner, sample size must be increased leading to increased laboratory workload. In addition, initial available cells or associated materials such as drug candidates can be limiting factors. Such limitations can be overcome by using LOC devices with integrated label-free biosensors.
Belonging to the electrochemical, more specific conductometric class of transducer principles, electrical impedance spectroscopy (EIS) is an analysis technique which facilitates non-invasive and time resolved measurements of cell cultures.
This measurement principle is sensitive to changes in cell-substrate interactions and therefore allows the monitoring of cellular dynamics such as surface adhesion, cell proliferation as well as morphological changes and cellular motility [43].

4.1.2.2 Explication of Electrical Impedance

In direct current (DC) driven circuits the opposition of a material to a flow of electrical current is denoted by its resistance (R) and is measured in Ohm (Ω). In alternating current (AC), the resistance of the system is given by the impedance signal (Z) which describes the relation between the electrical potential U and current I according to Ohm's law (Equation 2). In contrast to the resistance of a DC driven system, the impedance signal of an AC driven circuit has a complex character, composed of resistance and reactance.

$$R = \frac{U}{I}$$

Equation 2: Ohm's law, whereas R is the resistance (Ohm), U is the potential and I the current

Combined in the term reactance X, the inductance XL (voltages induced by magnetic fields of currents) and capacitance XC (stored electrostatic charges) form the imaginary part of the impedance (X = XL – XC) with j as the imaginary unit ($j = \sqrt{-1}$) and resistance R as real part:

$$Z = R + jX$$

Equation 3: Cartesian format of impedance.

Graphically Z can be depicted by displaying the real (Re) part on the x-axis and the imaginary (Im) part on the y-axis as shown in the Cartesian-coordinate representation in Figure 2.

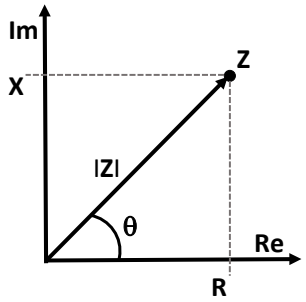

Figure 2: Cartesian-coordinate representation of complex impedance consisting of real (Re) and imaginary (Im) part.

Following the description in Figure 2, |Z| is calculated as:

$$|Z| = \sqrt{R^2 + X^2}$$

Equation 4: Magnitude of impedance signal |Z| short form.

and the phase Θ as

$$\Theta = arctan\left(\frac{X}{R}\right)$$

Equation 5: Phase of impedance signal

Due to its dependency on frequency changes, in contrast to resistance, the capacitive reactance Zc has to be considered as is given by:

$$Z_C = \frac{1}{2\pi f C} = \frac{1}{\omega C}$$

Equation 6: Capacitive resistance with C as the capacitance of a capacitor, f the frequency and ω the angular velocity

From the above equations the final calculation of the magnitude of impedance follows as:

$$IZI = \sqrt{R^2 + \left(\frac{1}{2\pi f C}\right)^2}$$

Equation 7: Magnitude of impedance |Z| long form.

4.1.2.3 Principle and Application of Electrical Resistance Measurements and Impedance Spectroscopy for Cell-based Analysis

Transepithelial electrical resistance (TEER) measurements allows to investigate the barrier integrity of cellular monolayers in terms of electrical resistance (Ohm). Schematically depicted in Figure 3 a is a classical TEER measurement setup composed of an insert with a semipermeable membrane immersed in cell culture medium and two electrodes, each on one side of the membrane. After applying an initial current across the membrane, the resulting current is measured and used to calculated the resistance based on Ohm's law (Equation 2). The resistance value then allows to gather insights in the quality of the cellular barrier which has formed on the semipermeable membrane.

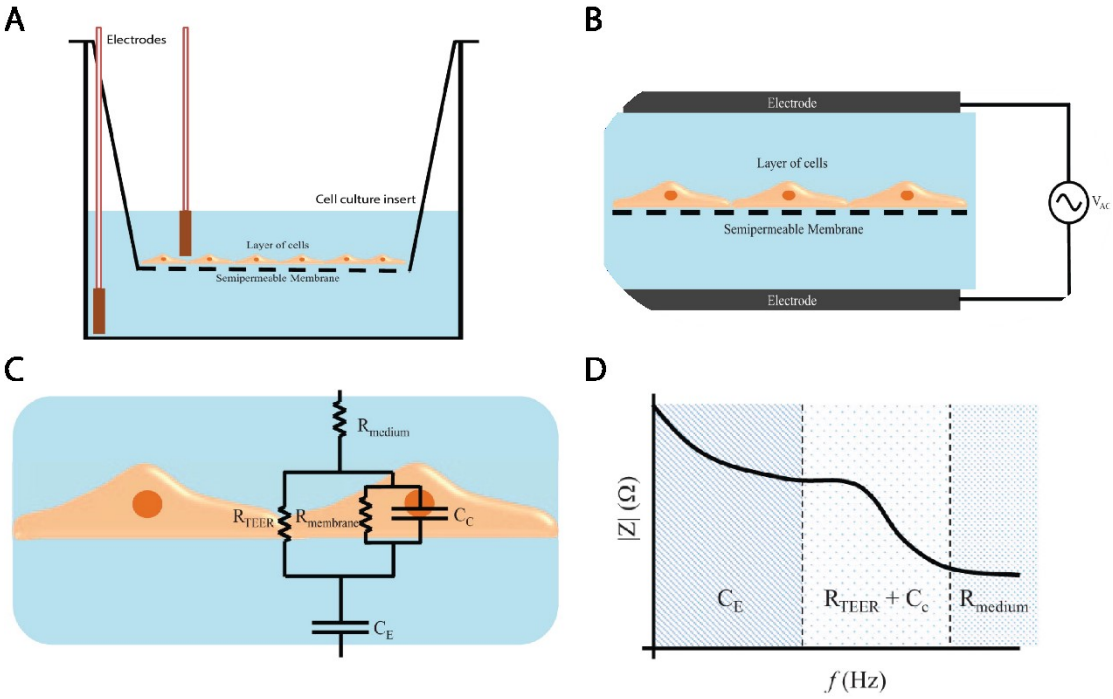

Figure 3: Concept of impendence based TEER measurements: (A) Schematic of a classical TEER measurement setup. Including an insert with a semipermeable membrane for culturing of cells immersed in medium with a cop stick electrode on each side of the membrane for applying current. (B) Schematic of TEER measurement setup for applying AC and plate electrodes for impedance spectroscopy measurements. (C) Resistance and capacity contribution to the impedance signal Z of various parts of the system. (D) Non-linear weighted contributions of resistance and capacity parts in dependence of a given frequency, adapted and with permission from Srinivasan *et al.* [44].

Today, most TEER measurement, instead of the initially used DC voltage, use AC voltage, since former can lead to cell damage and impairment of the sensors itself. The setup and working principle is similar but for DC, plate electrodes are used in place of cop stick electrodes as illustrated Figure 3B.
There a many commercial models available, varying in their electrodes and insert sizes. The Epiethelial Voltohmmeter (EVOM™) for example, allows to apply AC current at set frequency of 12.4 Hz and a resistance resolution of 1 Ohm [45].
However, instead of measuring resistance at a given frequency, impedance spectroscopy allows the recording of a whole spectrum of frequencies. This extends the capacity of recording changes in cells and cellular layers with regards

to the treatment. When applying AC, impedance is measured in means of amplitude and phase values. The impedance Z, therefore, not only gives information about TEER values but also about capacitive elements. Figure 3C describes the resistance and capacitive contributions of cell and medium to the resulting impedance signal Z.
Depending on the frequency, any resulting current can either take a paracellular-, or a transcellular path. Currents which pass paracellular paths, display the ohmic resistance, therefore measuring the transepithelial resistance (R_{TEER}). Allowing for information about the barrier integrity given by the arrangement of tight junctions between cells. For currents which pass transcellular paths, additional elements have to be taken into consideration. The lipid bilayer of a cell can be seen as a parallel circuit of resistance ($R_{membrane}$) and a capacitive (C_c) element. Furthermore, the resistance of the culture medium (R_{medium}) as well as the capacitance of the electrodes (C_E) must be taken into account when describing such models. Because of the resistance of cellular membranes, the current is usually forced to pass through the capacitive elements and that's why the resistance elements of cells are sometimes neglected when modelling such circuits.
The relationship of the non-linear frequency dependency of Z is depicted in Figure 3D. Simplified, the main contribution to Z at low frequencies results from the capacity of the electrodes whereas at high frequencies the resistance of the media becomes dominant, at mid-range frequencies TEER and capacity elements of the cells themselves are the main contributing factors [44].

A different form of impedance spectroscopy with the purpose of monitoring cellular behavior is the so-called electrical cell-substrate impedance sensing (ECIS, Applied BioPhysics inc, Troy NY, USA). In 1984 Giaver and Keese proposed their research on the topic [46], and in 1991 started to build up the company Applied Biophysics, which made this technology commercial available for a broad spectrum of researchers. Nowadays, varies research groups and companies, such as Roche (xCELLigenceTM) or Molecular Devices (CellKey) have adapted this technology and established their own arrays, varying in the geometry and layout of the electrodes, while employing the same general measurement principle.
The basic concepts are similar to the already described measurement technique, however here both the working-, and counter-electrode are in a planar arrangement with the cells growing directly on the sensor surface. The close proximity of cells and sensor results in a high sensitivity towards changes in cellular morphology. As such, these systems are greatly suited for studies on cancer migration and tissue invasion [47], cell-matrix interactions [48] as well as wound-healing studies [49].
Similar to the described TEER measurements, at low frequencies, cellular membranes represent a barrier to the applied current resulting in mainly paracellular flow.
However, by analysing a broad spectrum of frequencies, Wegner *et al.* have found that for monitoring cellular processes such as attachment, spreading and proliferation, measurements at frequencies around 40 kHz are most suited [48].

4.3 Retroviruses – a brief overview

The central dogma of molecular biology, firstly stated by Crick in 1958, describes the information flowing from DNA to RNA to Protein and was thought strictly unidirectional [50]. However, this dogma had to be reconsidered after the mechanism of retroviral replication was discovered. In brief, after the attachment and insertion of the viral RNA genome into the host cell, RNA is reverse transcribed into a DNA strand, via the viral enzyme reverse transcriptase. Afterwards, the genetic viral information can potentially integrate itself into the hosts genome where it can stay dormant for an unforeseeable time.

Retroviruses are usually in the size of 80 – 100nm in diameter with a 7-12kB long genome, which consists of two copies of a positive non-segmented single-stranded RNA molecule. A stable integration of the provirus into the host's genome entitle the viral information to be passively passed on from cell to cell with every division, often without adverse effects on the cells themselves. However, depending on the site of integration, there is a potential of activating so-called proto-oncogenes in the host cell's genome. These proto-oncogenes are often involved in regulating cell cycle, cellular growth and differentiation processes and can get upregulated upon the integration of a provirus. As the name suggest, these genes can promote tumour development, increase tumour growth and enhance metastatic potential [12]. The integration of retroviruses into the host genome can therefore have negative consequences for the cell, no effects at all or might even be beneficial. Part of the human genome consists of various endogenous retroviral sequences originating from infections which occurred generations ago. Some of those sequences can still be activated, as observed in early stages of the development of an organism. In early human embryogenesis, translated mRNA of such sequences protect the developing embryo from infections through viruses such as the influenza virus by modulating the innate immune system and associated proteins, hindering the attachment of a virus to the cell [51],[52].
The features of retroviruses were studied in depth which facilitated molecular biologist to developing and use them in cloning and sequencing techniques as well as gene delivery systems in gene therapy approaches [22].

4.3.1 Murine Leukemia Virus – A Simple Retrovirus

Retroviruses are classified by the shape and position of their internal core as well as by their genomic structure. One of the subfamilies of the retroviridae are the orthoretroviridae and within these we distinguish the genera alpha-, beta-, gamma-, delta-, epsilonretroviruses and lentiviruses. The largest group of gammaretroviruses are characterised by a condensed, spherical and central core known as type-C morphology as shown in the electron micrograph Figure 4.

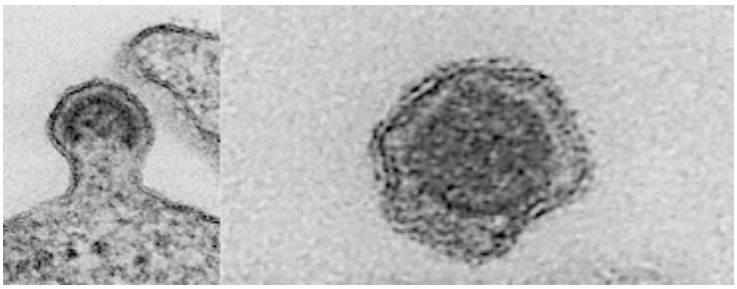

Figure 4: Electron micrograph of murine leukemia virus particle. The diameter of the particles corresponds to about 100nm. The virus has a typical type-C morphology and belongs to the genus of gammaretroviruses. Left: the budding of a new virion. Right: A mature virion (adapted and with permission from Copyright © 1997, Cold Spring Harbor Laboratory Press [22]).

4.3.1.1 Genomic Organization of Simple Retroviruses

Regarding the organization of the genomic structure, gammaretroviruses belong to the group of simple retroviruses. While complex retroviruses have sequences encoding for additional regulatory proteins, the genome of simple retroviruses only encodes for the most basic proteins required for a full replication cycle. These genes are gag, pro, pol and env, which encode for core structural proteins, viral protease, reverse transcriptase and integrase as well as the surface and transmembrane components for the viral envelope respectively. Figure 5 shows a schematic of the makeup of a typical simple retroviral particle [53].

As already indicated, the Gag gene encodes the structural components of the virion. The amino-terminal domain codes for the membrane associated, or matrix (MA) protein, and further for the largest of the structural proteins, the capsid (CA) with approximately 200-270 amino acid residues. The capsid protein encloses the viral ribonucleoprotein which together with the 60 - 90 amino acid residues long nucleocapsid (NC) build the core of the virion.

Three enzymes derive from the Pol and Pro polypeptides, the reverse transcriptase (RT), which has RNase H activity, the integrase and the protease. Together the reverse transcriptase and the integrase (IN) promote the reverse transcription of the RNA genome and the integration of the proviral DNA into the host's genome. The protease (PR) is responsible for cleaving the Gag and Gag-Pol polypeptide during the virion assembly, budding and maturation processes.

The specific attachment and penetration of a susceptible host cell is mediated by the transmembrane (TM) and surface (SU) subunits derived from the Env precursor polypeptide, which together build the envelope glycoprotein.

In this work, only simple retroviruses, with the emphasis on murine leukemia viruses (MLVs), will be discussed. As implicated by the name, MLVs have the ability to cause cancer foremost in murine but also in other hosts. MLVs are one of the most well-studied retroviruses and became the model system of choice. They were the first retroviruses modified and employed as gene delivery vectors and are still in use as the gold standard for viral clearance studies.

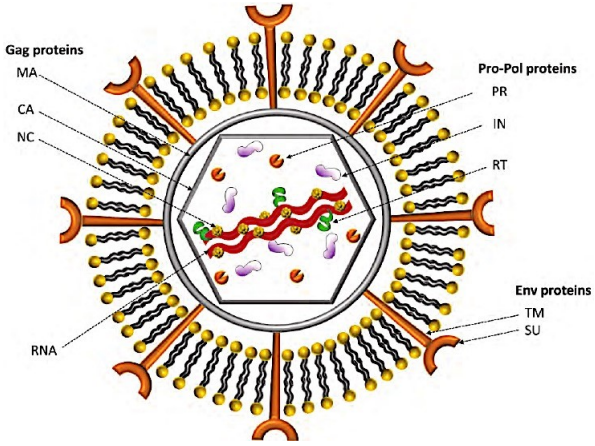

Figure 5: Schematic of a typical retroviral particle. In the centre the 2 copies of the linear RNA together with the gag-encoded structural core proteins MA (matrix), CA (capsid) and NC (nucleocapsid), are depicted. Also, indicated in the core are the pro and pol encoded proteins, the proteases (PR), and the enzymes, reverse transcriptase (RT) together with the integrase (IN). Encoded by the env gene, the TM (transmembrane) and the SU (surface) proteins, together with a lipid bilayer derived during the assembly and budding process from the host cells build up the viral envelope (adapted and with permission from © 2011 Rodrigues A, Alves PM, Coroadinha A. Published in [53] under CC BY 3.0 license. Available from: http://dx.doi.org/10.5772/18615).

For the reverse transcription of the RNA genome into a DNA molecule and the following integration as provirus into the host cell genome, the virus exploits the host cell's own machinery. As a result, the processed viral RNA contains a 5´cap structure and a 3´poly A tail. The organization of a typical retroviral genome is depicted in Figure 6. The genome is flanked by long term repeats (LTRs), or more detailed by terminal direct repeats (R) and the unique regulatory sequences at the 5´end (U5) and 3´ end (U3). The LTR on the 5´end acts as promotor for the host's cell polymerase II whereas the 3´ LTR constitutes as terminator for the transcription process and is further involved in the maturation of the viral transcript. Both LTR sequences are therefore crucial for the development of the provirus and its integration into the host genome. The primer binding site (PBS) functions as signal for the tRNA molecule and therefore acts as starting point of the reverse transcription. The polypurine tract (PPT), reflects the sequence responsible for the initiation of the positive strand synthesis during the reverse transcription. Finally, Psi (ψ) represents the packaging signal for the RNA molecules into the fresh virions [22].

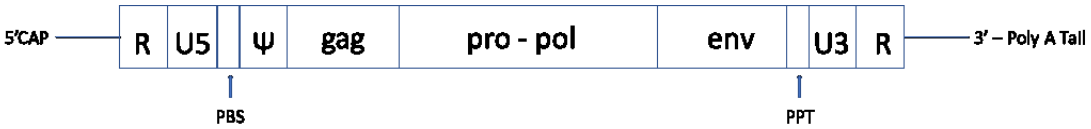

Figure 6: Representation of a simple retroviral genome. The terminal direct repeats (R) as well as the unique regulatory sequences on the 5´ (U5) and 3´ (U3) end, together with the primer binding site (PBS) and the polypurine tract (PPT) are involved in the regulation of the reverse transcription as well as in the integration of the provirus into the host genome. The psi (ψ) sequence act as specific signal for the packaging of the RNA into virions.

4.3.1.2 Replication Cycle of Retroviruses

The life cycle of a simple retrovirus, like the MLV encompasses several steps which are graphically summarised in Figure 7. They include the attachment to the host cell membrane, the entry of the nucleocapsid into the cytoplasm, the reverse transcription of the viral RNA into DNA, the integration of the provirus into the host cell genome, the transcription and translation of viral proteins and genomic RNA as well as the assembly, budding and maturation of the new viruses.

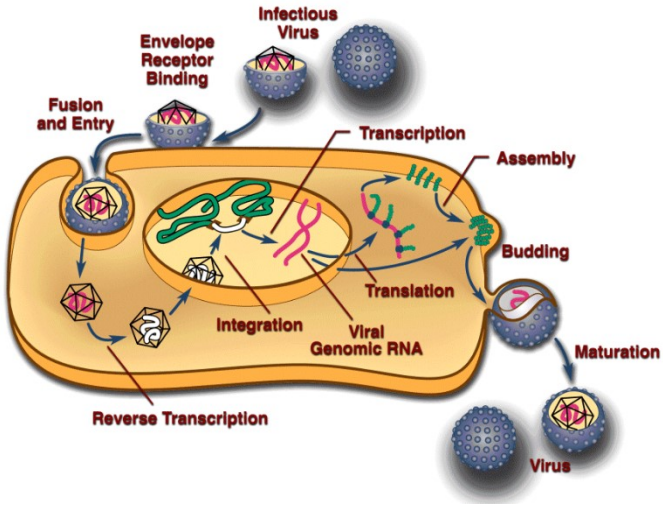

Figure 7: Representation of the life cycle of a simple retrovirus. Elucidated are the attachment and entry steps of the virus, the reverse transcription of the genome, the integration of the provirus into the host cell genome, the transcription of viral DNA, the translation of viral proteins as well as the assembly and budding of the newly synthesised virus and the later maturation (adapted from [54] and with permission from Elsevier and Copyright Clearance Center).

4.3.1.2.1 Attachment and Entry of the Virus

The attachment of the virus to the host cell membrane is the first step in a viral infection cycle. The initial step is mediated via the interaction of viral surface glycoproteins with specific membrane receptors of the host cell, which leads to membrane fusion, most likely through a conformational change within the viral transmembrane glycoprotein. Following the penetration of the cellular membrane, the viral core containing the genome and the reverse transcriptase enters the cytoplasm of the cell [54]

The cellular surface receptors and the pattern of viral surface glycoproteins determine the viral host range. Therefore, MLVs are classified into four host-range subgroups. Ecotropic MLVs, which only infect cells of mouse or rat origin. Xenotropic viruses, which are usually not able to enter cells of mouse origin although they are derived from endogenous sequences of inbreed mice. However, xenotropic as well as polytropic viruses can infect certain cells of wild mouse origin, such as *M. dunni* cells, in addition to cells of a variety of species other than mice. Amphotropic viruses, infect rodent cells as well as cells of other species including humans [55].

4.3.1.2.2 Reverse Transcription of the Viral RNA

The entry of the viral capsid into the host cell cytoplasm initiates the reverse transcription of the virus RNA, into a linear doubled stranded DNA molecule. This process includes several steps, during which the unique regulatory sequences (U5 and U3) at each end of the molecule are duplicated, allowing the formation of a linkage structure, necessary for the integration process of the provirus and later regulation of the viral gene expression. The resulting DNA molecule is similar to its RNA template, except for the duplicated regions (LTRs) as mentioned above, and indicated in Figure 8. After reverse transcription, the provirus is flanked by the two LTRs each consisting of a U3/R/U5 region. The transcription of this sequence ultimately results in a transcript, similar to the parental virus genome, which will subsequently be packed into new virus particles.

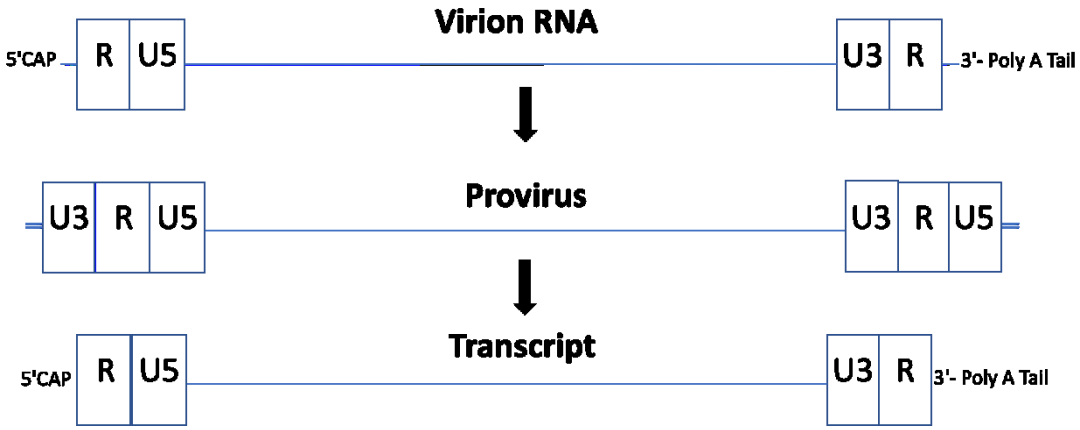

Figure 8: Representation of the virial genetic structure and elements during the cycle from the cytoplasm of a host cell to the integration into the hosts genome and the transcription of the provirus by the host cell machinery. Respectively, on top, the virion RNA with the flanking U5 and U3 sequences and the terminal direct repeats (R) are shown. After reverse transcription, the sequence of the provirus is extended by the duplication of the U5 and U3 regions, building the two LTRs with each a U3/R/U5 region. On the bottom, transcription of the proviral sequence, between the upstream U3 and the downstream U5 region, resulting in an RNA molecule like the original.

The reverse transcription and the duplication of the LTRs, are initiated by two different enzymatic functions of the viral RT. The DNA polymerase which can use either RNA or DNA as template and the RNase H which is an RNA-specific nuclease Figure 9represents the steps of the reverse transcription process schematically.
First the so-called minus-strand DNA synthesis is initiated by a host tRNA by binding to the PBS sequence of the viral RNA molecule. When the polymerase reaches the 5´ end of the template, a DNA intermediate of about 100-150 bases in length, the so-called minus-strand strong stop DNA (-sssDNA) is generated.
The RNase H activity then causes the degradation of the RNA:-sssDNA duplex which allows the -sssDNA to anneal to the 3´ end of the viral genomic RNA representing the first strand transfer. The transfer itself is mediated by the R sequences flanking both ends of the viral genome. When the -sssDNA anneals to the R sequences at the 3´ end of the RNA genome, the minus-strand DNA synthesis proceeds while the RNase H degrades the template strand.
Meanwhile, the PPT sequence of the viral genome is relatively resistant to RNase H mediated degradation and mediates the initiation of the plus-strand DNA

synthesis. After the plus-strand DNA is partialy generated, synthesis stops and results in the plus-strand strong stop DNA (+sssDNA) molecule.
After degradation of the tRNA primer the complementary PBS sequences are exposed allowing the +sssDNA and the minus-strand DNA to pair, which then results in the second strand transfer. Next, the synthesis of both strands is completed with each strand acting as template for each other.

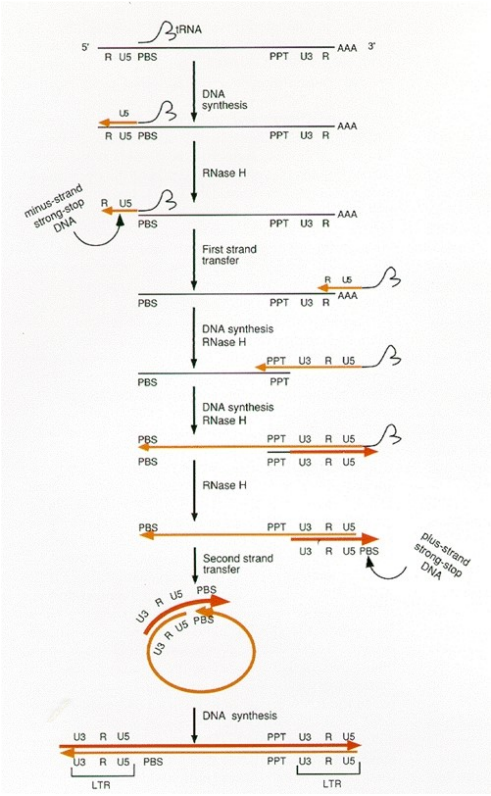

Figure 9: Overview of the reverse transcription process of a retroviral genome. (Adapted and with permission from Copyright © 1997, Cold Spring Harbor Laboratory Press [56].)

4.3.1.2.3 Integration of the Provirus into the Host Genome

While the reverse transcription of the viral RNA genome is prone to mutations, the integration of the provirus into the host cell genome reflects a stable integration and gives the virus sequence the status of a cellular gene. This results in the replication and transcription of the provirus by the cellular RNA polymerase II alongside the transcription of the chromosomal DNA.
In more detail, after the synthesis of the MLVs genomic DNA is completed, the molecule enters the nucleus of the cell. Before this process, the viral IN cleaves the 3´ termini by 2-3 bases, resulting in a 3´-OH group which acts as the attachment side to the host DNA. Together with compounds of the virion core and most likely together with some cellular proteins, it forms the so-called pre-integration complex.
The provirus of MLVs, in contrast to other retroviruses like for example HIV or lentiviruses, can only enter the nucleus of the cell during mitosis, when the nuclear membrane is broken done. After formation of the pre-integration complex and the association with the host cell DNA, the IN catalyzes a transesterification reaction, which ultimately leads to integration of the viral DNA. The side of integration is

not random, but locations are widely distributed throughout the host cell DNA. After the integration, gaps and mismatches are filled and corrected by DNA synthesis processes, most likely mediated by the viral RT. The last step of the integration of the proviral DNA consists of a ligase step and the disassembly of the pre-integration complex.

4.3.1.2.4 Transcription, Synthesis and Assembly of Viral Proteins

Since the integrated provirus is indistinguishable from a cellular gene, its transcription and RNA processing also rely on the host cell machinery. The LTRs of the provirus play a crucial role and act as cis- elements for the recruitment of cellular proteins and control elements to facilitate the transcription process and posttranscriptional processing of the RNA product respectively.

Following transcription via the host cell RNA polymerase II, the viral RNA transcripts are modified with a 5´ cap and a 3´ poly A tail structure identical to cell's own transcripts. This ensures that the cellular machinery recognises the transcripts for further processing without degrading them. The resulting viral transcripts are either full-length transcripts, which resemble the genomic RNA of the virus and also can act as template for Gag and Pol protein synthesis, or they are sub-genomically sized, and function as mRNA for the synthesis of the remaining viral proteins.
The load of viral RNA within a host cell varies among the virus species and their specific host range but also depends on the differentiation status and activity of the cell itself. The viral RNA load of MLVs within an infected JLS-V9 cell culture for example can be around 5 – 10% of the cells total mRNA [57].
The transport of the viral transcripts from the nucleus into the cytoplasm is most likely associated with heterogeneous ribonucleoprotein particles (hnRNPs), which act as chaperones for the mRNAs or by the binding of 5S ribosomal RNA to the TFIIIA transcription factor which facilitates the export out of the nucleus [58].
The process of the assembly of viral proteins and genomic RNA into functional virions is not yet fully understood due to the differences within the virus species themselves
After the translation of the viral transcripts by the ribosomes, the polypeptides are processed and assembled via the rough endoplasmic reticulum and the Golgi apparatus and next transported to the cellular membrane. During this process, the single compounds (SU, TM, MA, CA, NC, PR, RT and IN) are cleaved by cellular and viral proteases and undergo various maturation steps. Vesicles containing the viral proteins and genomic RNA are brought to the side of budding where they are assembled into new virions. It is known that the Gag protein is crucial for packaging and budding events of the newly synthesised viral particle. It has been shown that even in the absence of all other viral proteins, above steps are initiated and viral-like particles bud off the cellular membrane. Therefore, the main packaging signal (ψ) has to be located within the Gag protein domain [59]. Besides the viral proteins, the infectious particle also requires cellular tRNA, which is packed into the virion in association with the viral RT [60]. After budding of the viral particles, the last maturation step, forming full infectious viruses is accomplished. This step is mainly a condensation step of the Gag, and Gag-Pro-Pol proteins by the viral PR [61].

4.3.2 Retrovirus for Therapeutic Approaches

4.3.2.1 Retroviral Vector-based Gene Therapy

Retroviruses were studied intensively for their suitability as gene delivery systems to treat various monogenetic diseases. Due to their stable integration into the host chromosome, their genome is transmitted with every cell division which make them uniquely attractive for named approaches. For safety reasons, retroviral vectors are rendered replication-deficient and need a "helper" virus for the completion of their replication. Tabin et al., used MLV as vector system, for the transmission of the herpes simplex viral thymidine kinase into animal cells by replacing the virus genome partially with the target gene and by utilizing a helper virus [62]. Despite the relative safety of a replication-deficient retrovirus, recombination events can still occur leading to a once more replication-competent virus. Since this process occurs randomly and has the potential to cause unwanted retroviral spreading, potentially even causing cancer, such a system was quickly disregarded.

Soon after realizing above disadvantages, packaging cells were introduced, and various cell lines were established covering a broad spectrum of species. In this new approach, all genes necessary to propagate are usually removed from vectors. The first and one of the most frequently used vector systems at the time are MLV-based vectors. In these, often only cis acting sequences such as LTRs, PBS, PPT and ψ remain and a therapeutic gene is inserted. The packaging cell line contains the genes for the viral capsid as well as those necessary for the maturation of the virus-based vector. The resulting vector particles are than collected and introduced into target cells [63].

Gene therapy approaches not only include the goal of correcting monogenetic disorders but also extend to therapeutic strategies for cancer and infectious disease treatment such as HIV. In the first clinical trial of human gene therapy, beginning in 1990, an MLV based gene delivery vector was used to transmit human adenosine deaminase (ADA) cDNA into mature peripheral blood lymphocytes of two ADA-deficient patients. Ten years after the last treatment, in one patient, 20 % of the lymphocyte still carried the viral gene but only less than 0.1% showed transgene expression. In the second patient, no transgene expression was found. Thus illustrating the putative longevity and potential safety of the viral sequences within those cells, while also revealing difficulties of gene therapy approaches [64].

However, the process of integration of parts of the retroviral genome into the host genome can lead to activation of cellular proto-oncogenes or suppression of tumor suppressor genes. Such events, termed insertional mutagenesis, though extremely rare, could still occur when retroviruses are used as vectors and therefore such strategies remain risky. Nowadays, further safety strategies are introduced and different vectors such as lentiviral-based systems are exploited. Lentivirus in contrast to retrovirus can also infect non-dividing cells and therefore extending the range of applications. Morgen *et al.* give a comprehensive review of the beginnings and the development of vector based gene therapy up to now [65].

4.3.3 Retroviral Detection and Quantification Methods

With the variety of existing viruses comes also a variance of virus detection and quantification methods. Each tailored to investigate a different aspect of a virus family or the lifecycle of a virus. The methods used for investigations of a certain virus usually depend on observably cytopathic effects caused by the infection process itself and on the intent of determine only the presence or also the quantity and infectivity potential of the viral particle. In the following sections, some of the most commonly used assays and their specification are described.

4.3.3.1 Plaque-Assay

The classical plaque assay also referred to as infectivity assay is used to determine the concentration of infectious virus particles within an unknown sample. Therefore, a series of dilutions of the virus-containing fluid is prepared and added to a susceptible cell layer. After the infection of a cell, new virus particles are formed and spread to the neighbouring cells, where this process is repeated, and the virus spreads to the next cells. Since this assay is based on cytopathic events of cells following an infection, the resulting effects can be observed by the consecutively formation of empty spots or more commonly plaques. As an additional step, the cell layer is often covered by a semisolid layer post infection. Thus, allowing the adequate supply of nutrients while hindering the unintended spreading of newly formed virus to other neighbouring cells. Thereby falsified outcomes can be avoided. After a cell- and virus-specific culture period, which usually takes 3 to 14 days, the cell layers are fixed and stained to enhance the contrast of the remaining cell layer to the empty plaques. The virus concentration is then determined by counting the plaques and the dilution factor used to prepare the medium with which the cell cultures where inoculated. The results are usually represented as plaque forming units per millilitre (PFU/mL) [66]. However, one commonly observed drawback, is the tendency of obtaining low plaque counts. This can be a result of not all infectious particles actually infecting a cell but also due to the possibility that infected cells are not far enough apart, fuse and therefore are not counted separately. This problem is mitigated by performing a dilution series and averaging several infected cell cultures with the cost of making this assay more labour-intensive.

4.3.3.2 50% Tissue Culture Infective Dose (TCID50)

The 50% tissue culture infective dose (TCID50) assay is a similar endpoint assay to the plaque assay. In contrast to the plaque assay, no exact virus concentration is determined, instead the intent is to specify the virus dilution by which half of the cultures show cytopathic effects. Therefore, after an appropriate culture time, the cell layers are analysed as a whole and only investigated on the regards of if they show any cytopathic effect or not. With this protocol, the potential of false outcomes due to unintended spread of newly formed viruses, as often observed in the plaque assay, can be eliminated [67]. Importantly, the PFU/mL and the TCID50 values cannot be used interchangeably due to differences in the respective assay protocols.

4.3.3.3 Fluorescent Focus Assay (FFA)

The fluorescent focus assay is based on the same concept as the plaque assay with regards to inoculating cell cultures with a dilution series of virus containing

medium. The detection of CPEs in the cultures however is accomplished by fluorescence microscopy. After only 24 to 72 hours, the cultures are exposed to fluorescently labelled antibodies specific to the virus of interest and the positive stained cells are counted and fluorescent focus forming units (FFU/mL) can be calculated. This assay generates data faster, however the costs for reagents, equipment and time needed to observe and count the positive stained need consideration [68].

4.3.3.4 Hemagglutination assay & Hemagglutination inhibition assay

There are two variants of the hemagglutination assay (HA). The first one is based on the formation of red blood cell clots after the viral protein hemagglutinin is brought into contact with them. Similar to other assays, a dilution series is prepared and added to a defined number of red blood cells. The results can be obtained already after 1-2 hours and are depicted in hemagglutination units (HAU). The second variant is based on the inhibition of the clotting process of red blood cells. In the hemagglutination inhibition assay (HI), antibodies against the virus are added to the culture medium which then interfere with the binding process of the virus to the red blood cells and thereby inhibit the formation of clots. These assays yield fast results but are error-prone due to variations of red blood cell concentration, the potential of other reagents causing the blood cells to clot and variations in the interpretation of the results [69].

4.3.3.5 Bicinchoninic acid assay (BCA)

The bicinchoninic acid assay (BCA) is a protein-based assay for the detection and quantification of viruses. The principle of the assay relies on the reduction of Cu^{2+} to Cu^{+} by peptide bonds of proteins. Afterwards, bicinchoninic acid molecules can bind the Cu^{+} which results in the formation of a coloured complex. The change in colour is determined by spectrometric methods and is proportional to the amount of proteins present. By comparing to a protein standard curve, the total protein content can be calculated. Consequently, special care has to be taken to avoid high contamination by host cell proteins [70].

4.3.3.6 Enzyme-Linked Immunosorbent Assay (ELISA)

The ELISA assay represents another colorimetric-based protein detection method. The first step is to link specific antibodies on the surface of a, usually 96-well plate. In the second step, the sample to be analysed is added to the wells, which will bind to the immobilised antibodies. In a third and fourth step a secondary antibody specific to the protein is added usually tagged with an enzyme. After a washing step, substrate is added and gets converted by bound antibodies carrying the enzyme. This is accompanied by a change in colour of the substrate which is then measured. The general make-up of this assay allows for high variability in the form of combinations of antibodies and antigens and depend on the protein in question. The assay itself is highly sensitive and can detect proteins down to picomolar and nanomolar concentrations.

4.3.3.7 Quantitative Polymerase Chain Reaction

The quantitative polymerase chain reaction (qPCR) is based on the amplification of DNA sequences. Primers which specifically bind to the beginning and end of a sequence of interest are designed, allowing the polymerase to bind and start the

synthesis of new complementary strands. The monitoring of a fluorescence signal which increases logarithmically as a result of the ongoing duplication of new DNA-strands over a set of temperature cycles allows for this highly sensitive detection method. There are variations of how fluoresce dyes interact with the DNA. Usually it is based on an intercalating dye which gives a signal as soon as double stranded DNA is present or by the binding of a fluorescently labelled probe, specific to a certain DNA sequence. The increase in fluorescence signal is proportional to the amount of DNA molecules present in the sample which allow the calculation of initial concentrations by comparing it to a standard curve. The sensitivity of this method allows to detect very low amounts of DNA molecules. However, it does not allow to distinguish between infectious and non-infectious particles.

4.3.3.8 Product enhanced reverse transcriptase assay (PERT)

Product enhanced reverse transcriptase (PERT) assay also termed as Amp-RT is based on the detection of retroviruses by using the activity of the viral reverse transcriptase. In a first step, the potential virus containing sample is mixed with a virus lysing reagent and thereby releasing viral reverse transcriptase. A suitable RNA template and according primers are added to allow the viral reverse transcriptase to transcribe the RNA template into cDNA strand. Since its first development, improvements and enhancements lead to variations specifically in the signal detection of the assay. The original assay protocol used radio-labelled nucleotides which were incorporated into the DNA strands and afterwards could be detected by a radioactive sensitive film [71]. As an alternative, more modern versions include a polymerase chain reaction-based amplification step after the initial transcription often in combination with the incorporation of for example 5-bromo-deoxyuridine-57-triphosphate (BrdUTP) instead of thymine. This can then be used to detect the product through a colorimetric enzyme-immunoassay [72],[73].

4.3.3.9 Flow Virometry

Another method used to detect viral particles is based on flow cytometry and is termed virometry. Virus particle can the detected in samples stained against virus-specific proteins in combination with a staining for nucleic acids. The sample solutions flow through a fluidic channel which passes a laser beam. If the specific staining are present the signal can be detected, and the concentration is calculated and given in virus particles per millilitre (vp/mL) [74].

4.3.3.10 Transmission Electron Microscopy

Transmission electron microscopes not only allow nanometre resolution but can also be used to quantify virus particles. However, only very thin samples can be imaged, and sample preparation is very time-consuming. Transmission electron microscopy is often used to analyse the shape and specifics of viruses. However, if the method is used for quantification purposes the results are displayed as well as vp/ml. Flow virometry as well as transmission electron microscopy are cost intense in purchase as well as in maintenance and therefore often not the first choice as viral detection and quantification method.

4.3.3.11Molecular Imprinted Polymers (MIP) and Quartz Crystal Microbalances (QCM)

Molecular imprinted polymers represent not only an alternative for antibody, antigen or enzyme-based approaches such as ELISA assays but can be used to detect a variance of other, mostly biological molecules. MIPs are relay on receptor – target interaction mainly based on shape recognition, involving electrostatic interactions, hydrogen bonds, Van der Waals forces and hydrophobic interactions but can also rely on covalent interactions and depends on the fabrication method of the MIP. In the most basic technique, imprints are often generated by pressing the molecule of interest into the semi-solid polymer and remove it after polymerization. This leads to an exact imprint of the target molecule and can be later used to capture the target species out of a pool of molecules. Today highly sophisticated imprint techniques exist and are used detection of chemical pollutants, drug residues, heavy metals or viruses. Mingkun *et al.* give an comprehensive overview of fabrication techniques and modern applications for MIPs [75]. Quartz crystal microbalances are highly mass-sensitive sensors and react to frequency changes of the resonance of a quartz crystal. Electrodes on both sides of the piezoelectrical plate allow the application of AC voltage. Put simply, the method allows the monitoring of changes in acoustic resonance resulting from changes in mass. This concept was first described in 1964 [76], and has applications for e.g. sensing allergens [77], analysing carbohydrates [78] or microorganisms in general [79]. A combination of MIP and QCM technologies enables highly specific receptor-target interaction detection with a highly sensitive analysis method.

4.4 Background in Cell Lines and Chosen Virus

4.4.1 Background in the *M.dunni* Cell Line

In 1984 the *M. dunni* cell line (Clone IIIC8) was isolated from the tail skin of a wildtype *Mus terricolor* and possesses fibroblast-like morphology. They cell line is regularly used for the amplification of MuLV of all classes [80] .

4.4.2 Background in the PG-4 Cell Line

PG-4 cells have an astrocyte-like morphology and originate from cat brain cells (G355). The cell line is Moloney sarcoma transformed and harbours a Murine Sarcoma virus genome which is defective in part of the envelope proteins. The defective genome of the sarcoma virus can get rescued after superinfection with for example the xenotropic murine leukemia virus. During virus particle propagation, PG-4 cells tend to round up and detach from the surface, which leads to the classical formation of plaques within a confluent cell layer. Plaques therefore are areas with rounded or no cells surrounded by so far morphologically intact cells [81].

4.4.3 Background in Xenotropic Murine Leukemia Virus

The xenotropic murine leukemia virus (x-MuLV), strain pNFS Th-1, belongs to the family of retroviridae and the genus of gammaretroviruses. It was isolated from the thymus of a 5.5-month-old NFS swiss mouse by JW Hartley and published in 1977[16]. Since being characterised as a xenotropic virus, it usually does not lead

to a disease in the host species but can infect other species and leads to plaque formation on PG-4 (feline S+L-) and foci of rounded cells on MiCL1 (Mink S+L1) cell lines. As described before, this virus was derived from endogenous sequences of inbred mice, it does not exogenously infect mouse cells, except for certain cells of wild mouse origin, such as M.dunni cells [16];[82].

5 Materials and Methods

In the Material and methods section of our published work (pages 1365 – 1367); [21], the following parts are described:

- Chip design and Fabrication,
- Bioimpedance spectroscopy,
- Cell culture handling,
- One-chip cultivation – extended infectivity protocol,
- Flow cytometry – Cell cycle analysis
- qPCR – virus sample preparation and
- Computational fluid dynamics – fluid modeling

5.1 Infectivity Assessment using Plaque Assay

To assess the TCID50 values of virus stocks and thereby excluding changes in infectiousness of the X-MuL Virus due to storage conditions, off-chip plaque assays where performed regularly. Therefore PG-4 cells were seeded into 48-well plates (PAA) at a concentration of 1,5 x 10^4 cells/ml. After 24 hours virus stock dilutions ranging from –log1 to -log6 where prepared in 0,5 log steps and added to the cells. At day 7 after seeding the PG-4 cells were washed with PBS and fixated with Accustain Formalin Free Fixative (VWR) for 1 h, followed by a 15 min Accustain Crystal Violet staining (5%) in 20% Ethanol (VWR). The TCID50 values were calculated using the Karber Calculation.

6 Results

6. 1 Investigation of Drug-free Cell Cycle Synchronization Methods for *M. dunni* and PG-4 cells

For a successful integration of retroviral DNA, the timing of exposure to the virus is important. The time critical window for most cell lineages is 12 to 24 hours after entry of the virus. Proliferating cells are reaching their next mitosis phase which includes the breakdown of the nuclear membrane and allows the viral DNA to integrate in the hosts genome. For the establishment of the assay protocol it is therefore crucial to obtain a synchronised cell culture, 12 – 24 hours prior to mitosis, to achieve high infection levels. The cell cycles of *M. dunni* and PG-4 cells were analysed using FACS, to identify the timepoint in which the majority of cells cycle through the G2/M phase. Three culture conditions were investigated, cells cultured in full culture medium, cell starved for 48 hours by culturing in medium lacking FCS or cells which were released from 48 hours starvation period. As described in our published work, (Figure 4, [21]), no enhancement of cell

population in G2/M phase could be achieved by last two culture methods. In the following chapters, the obtained results are described in more detail.

6.1.1 G1 Phase Synchronised Cell Population by Enzymatic Cell Detachment and G2/M Phase Population Peaks at 13 and 26 hours after Cell Seeding

As depicted in Figure 4A of our publication [21] and Figure 10 in this manuscript, *M. dunni* cells cultured in full medium, showed a cell population of almost 80% in G1 phase. This effect can be attributed to the enzymatical induced cell - substrate detachment. Between 6 and 13 hours after cell seeding, the culture re-enters the proliferative state, resulting in a up to 32.6% of the total cell population in G2/M phase. Within the following 17 hours, the G2/M phase population maintains similar values and shows a second increase in G2/M phase values 13 hours after the first, at 26 hours after second cell seeding. Afterwards, G1 phase cell population increased and S and G2/M phase populations continually decreased.

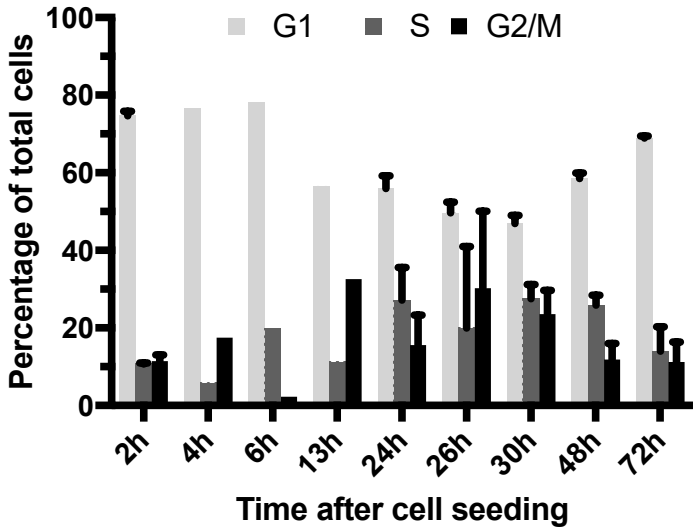

Figure 10: Analysis of cell cycle populations after enzymatically induced synchronization using FACS: *M. dunni* cells cultured in complete growth medium over 72 hours, (adapted from [21]).

6.1.2 Cell Population Synchronization by Serum Starvation

A common method to induce non-chemical cell synchronization is the culturing of cells in low or even FCS free medium. As a control group to cells released from serum starvation, *M. dunni* cell cultures were monitored over a 48 hours starvation period. After a 2 hours adaption phase of the cells in full culture medium, it was replaced by a serum free medium. Serum-starved cells showed a continuously high percentage of cells in the G1 phase of the cell cycle compared to the whole observation period. Results depicted in Figure 11 show values of about 80% over the first 13 hours with a slight decrease to 63,8% at 24 hours. The population increased to 77,8% 72 hours after cell seeding. Lower levels of G1 phase positive cells between 24 and 48 hours where accompanied by three times increase of G2/M phase population 13 hours after conditioning had started as well as the increased percentage of S-phase cells.

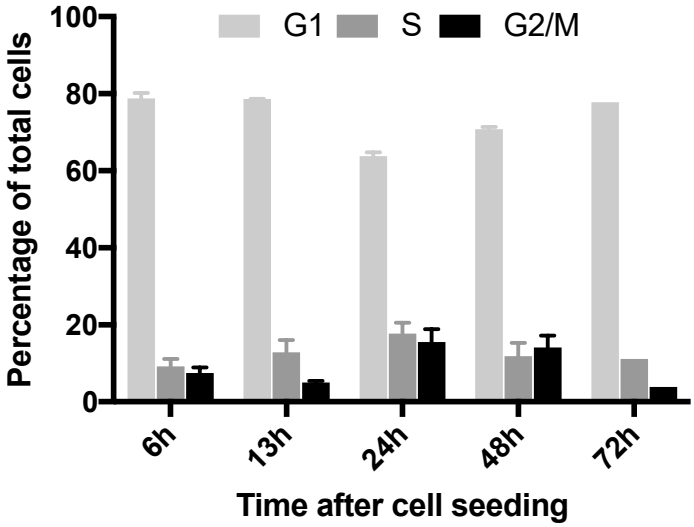

Figure 11: Effect of serum starvation on cell cycle: *M. dunni* cells where cultured in their complete growth medium for 2 hours after which the medium was exchanged to a serum free one. The population of G1 phase cells over the first 13 hours shows a stable average value of 78,6%, decreasing to 63,8% after 24 hours after which the population increased to 70,8% at 48 hours and 77,8% after 72 hours. Cells population of G2/M cells ranged from 7,5 at 6h to 5% at 13 h over 15,5% and 14.1% at 24 h and 48 h to 3.9% at 72 hours after cell seeding. The S-phase cells population was at a value of 9.2% at 6 hours, 12.9% at 13 hours, 17,7% at 24 hours, 11,8% at 48 hours and 11.1% at 72 hours after cell seeding.

6.1.3 Re-entry of cells into proliferative cell cycle after a 48 hours starvation treatment is effective for cell synchronization

In the third method, the re-entry into the normal cell cycle of proliferating *M. dunni* cells was investigated after a 48 hours starvation period. After the FCS-dependent starvation period the cells were cultured in complete growth medium and samples were analysed after 4, 6, 12 and 22 hours of culture time. As depicted in Figure 12 over the first 6 hours, up to 75,2% of cells were in G1 phase. Interestingly, 4 hours after the release of the cultures from the starvation, 22% of the total cells were in G2/M phase, after which this fraction decreased to 8,8% at 12 hours and again increased to 12,4% at the 22 hours sampling timepoint. The fraction of S-phase cells was low over the first 6 hours at 2,3% to 7,3% after which the population increased to 31% at the 22 hours timepoint.

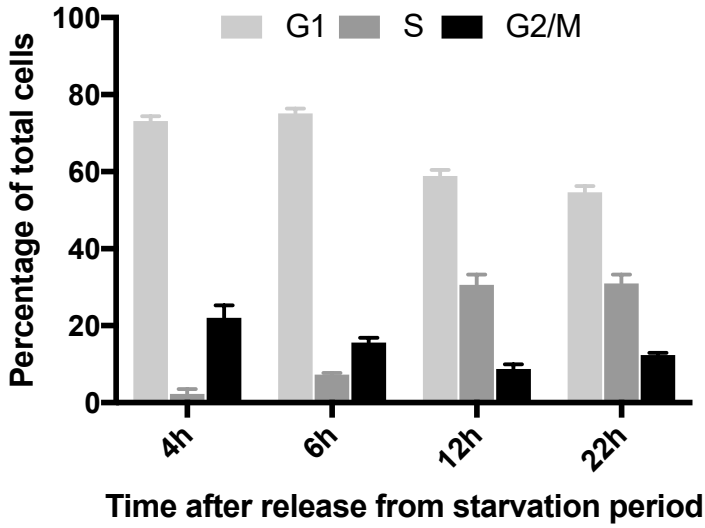

Figure 12: Re-entry of starved *M. dunni* cells into proliferative state: Cells where serum-depleted for 48 hours after which they were allowed to re-enter cell cycle by providing the culture with complete growth medium. Over the first 4 to 6 hours the 73,1% and 75,2% of the total population of cells where in G1 phase. Thereafter the fraction decreased to 58,9% at 12 hours and 54,7% at 22 hours. The cell population of G2/M cells was highest 4 hours after releasing the cells out of serum starvation with a value of 22%, and then decreased to 15,7% at 6 hours to 8,8% at 12 hours after which it increased to 12,4%. The fraction of S-phase cells continuously increased over time from 2,3% at 4 hours 7,3% at 6h 30,7% at 12 h and 31% at the 22 hours sampling timepoint.

6.1.4 Determination of Cell Cycle Perturbations of the PG-4 Indicator Cell Line due to *M. dunni* Synchronization Protocols

The DNA content of both *M. dunni* and PG-4 cells was investigated after the application of the different cell cycle synchronization protocols. Figure 13 shows the data of all three approaches, culture in full medium (A), culture during a starvation period (B) and the culture after the release from a starvation period (C). This showed a constant high cell population in G2/M phase regardless of the cultivation method.

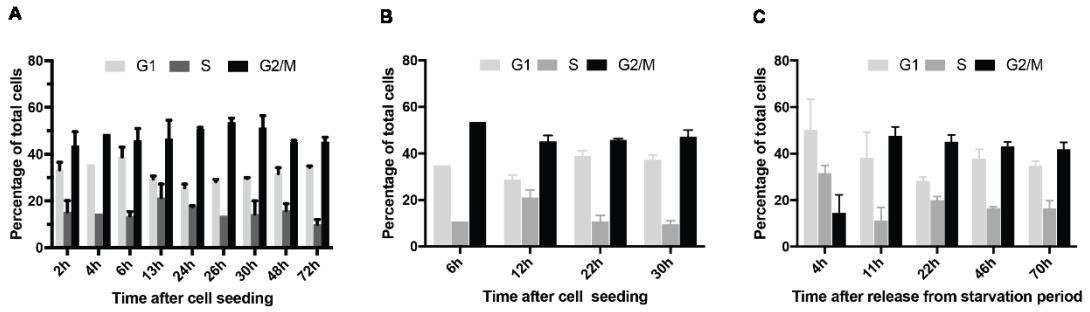

Figure 13: Investigation of cell cycle arrest or synchronization events depending on cell culture protocol: Graph A also shown in paper shows PG-4 cells cultured in full growth medium over the time period of 72 hours. Graph B shows the result for PG-4 cells starved for 30 hours by serum depletion and Graph C show the results of PG-4 cells at various time points up to 70 hours after cells where starved for 48 horus and then released out of a potential arrest by exchanging the medium to a complete growth medium.

6.2 Time-resolved Monitoring of x-MuLV Particle Release from Infected *M. dunni* Cultures

The majority of results of the presented work was published in February 2021 in the Journal Lab on a chip and is incorporated in the end of this section [21],[83]. In addition to the results already published, ESI† Fig. S4 [83], of inoculating *M. dunni* cell cultures with a virus titre of 7.7 × 10^3 PFU /ml, 12 hours after cell seeding, experiments with inoculation time points at 6 hours and 26 hours after cell seeding with a virus titre of 2.2 × 10^5 PFU /ml, where performed. We monitored the release of the virus particles of the course of 72 hours.

For *M. dunni* cultures which were exposed to the virus 6 hours after cell seeding, x-MuLV particle values detected by qPCR analysis, showed an initial drop in the first 18 hours of culture. Thereafter a constant increase of detectible virus particles was observed as seen in
Figure *14*. Between 36 - 54 hours after inoculation, the PFU /ml had more than doubled (576 – 1379) and reached a value of 10,976 PFU/ml after 72 hours.

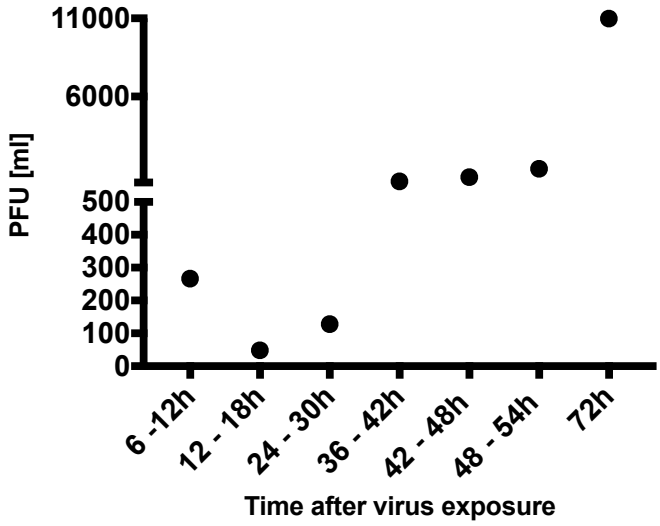

Figure 14: Determination of PFU/ml in supernatant of *M. dunni* cell cultures inoculated with an initial virus titre of 2.2 x 10^5 PFU/ml, 6 hours after cell seeding.

M. dunni cultures exposed to the x-MuLV containing media (2.2 x 10^5 PFU/ml), 26 hours after cell seeding displayed a steady decrease in detectable virus particles as seen in Figure 15. From an initial value of 529 PFU/ml, 6 – 12 hours after exposure the PFU /mL dropped to 7 after 72 hours of culture period.

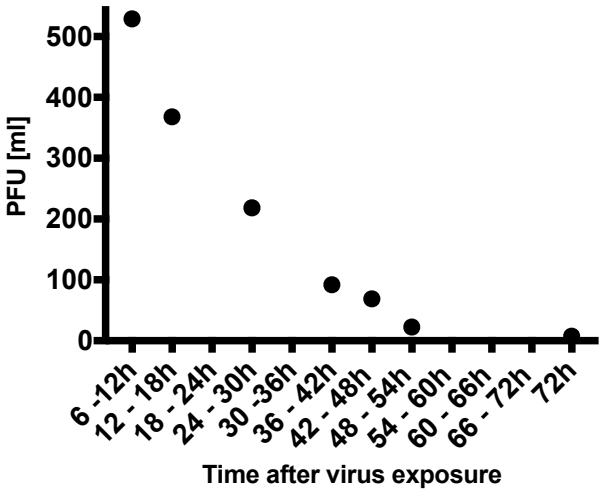

Figure 15: Determination of PFU/ml in supernatant of *M. dunni* cell cultures inoculated with an initial virus titre of 2.2 x 10^5 PFU/ml, 26 hours after cell seeding

6.3 Impedance-time Traces of *M. dunni* Cultures for Assay Performance Control

M. dunni cell cultures responded with a sustained biphasic adhesion and spreading behavior, reflected in the representative impedance-time traces of control cells shown in Figure 16A (dark grey). However, this pattern loses its prominence when cultured coupled to PG-4 cultures (light grey).

While in uncoupled *M. dunni* culture, a plateau is reached about 65 hours after cell seeding; strikingly, when coupled to PG-cells a steady increase of averaged 0.6 Ohm/h was observed. In Figure 16B, both control impedance-traces are compared to an impedance-trace of dying *M. dunni* cells (black trace). negative-outcome example represented by the black trace. The sharp decrease of the impedance signal, after 15 hours of culture period averaged 2 Ohm/h and reflects a dying *M. dunni* cell culture, precipitated by lowering the overall temperature of the culture platform.

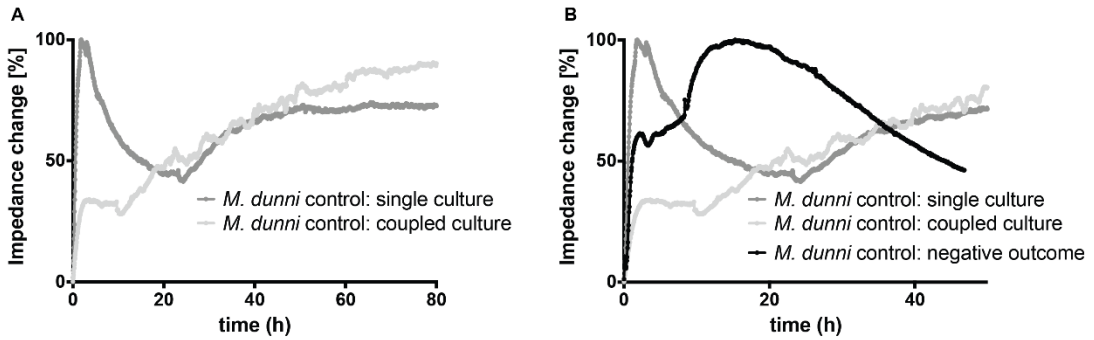

Figure 16: Characteristics of impendence time traces: (A) Single *M. dunni* cell culture compared to cultures coupled to PG-4 cell culture. (B) Impedance time traces from A compared to a dying *M. dunni* cell culture.

6.4 Extended Infectivity Assay Performance Evaluation at Lower Initial Virus Infection Doses

For the establishment of the extended infectivity assay protocol a virus titre of 2.2 x 10^5 PFU/ml initial virus titre was used. Next, the robustness of the assay protocol was investigated. Initial virus titres were reduced in log steps and ranched from 1.05 x 10^4 to 1.05 x 10^2 PFU/ml. As an experimental control set the potential cytopathic effects of lower virus titres were tested on single PG-4 cultures only which were infected at the timepoint of seeding.

6.4.1 Impedance-time Traces of Single PG-4 Cultures infected with Low Virus Titres

In Figure 17, the impedance-time traces of PG-4 cultures infected with 1.05 x 10^3 (dark grey) and 1.05 x 10^2 PFU/ml (light grey) at the timepoint of seeding were compared to a uninfected PG-4 control culture (green). The PG-4 culture infected with 1.05 x 10^2 PFU/ml showed no detectible cytopathic effects according to the impedance trace over the course of 70 hours In contrast, the culture infected with 1.05 x 10^3 PFU/ml displayed a typical growth curve over the first 60 hours followed by a decrease in the impedance signal over a period of 10 hours after which it once more increased.

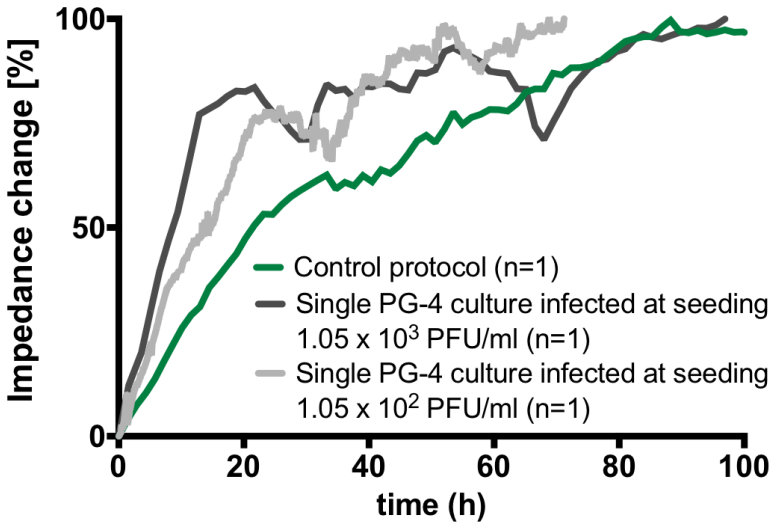

Figure 17: Comparison of control PG-4 culture to low level infected cultures: Non-infected PG-4 culture (green) in comparison to PG-4 cultures initially infected with a virus titre of 1.05 x 10^3 PFU/ml (dark grey) and 1.05 x 10^2 PFU/ml (light grey).

6.4.2 Performance Evaluation of The Extended Infectivity Assay with Various Initial Virus Titres

The previous set of experiment confirmed that at lower virus titres, the potential CPEs on the cell culture are not severe enough to be clearly detectable by the implemented sensor system. Therefore, in next step, the extended infectivity assay protocol was applied in combination with lower virus titres to evaluate its robustness. Figure 18 shows the control culture (green) compared to the impedance trace of a PG-4 culture connected to a *M. dunni* culture (black) initially infected with 1.05 x 10^2 PFU/ml for viral amplification, according to the established protocol. After 65 hours assay time, the impedance values started to

rapidly decrease, which is in accordance with the previous experiments at higher virus titres, conforming CPEs on the PG-4 cell culture.

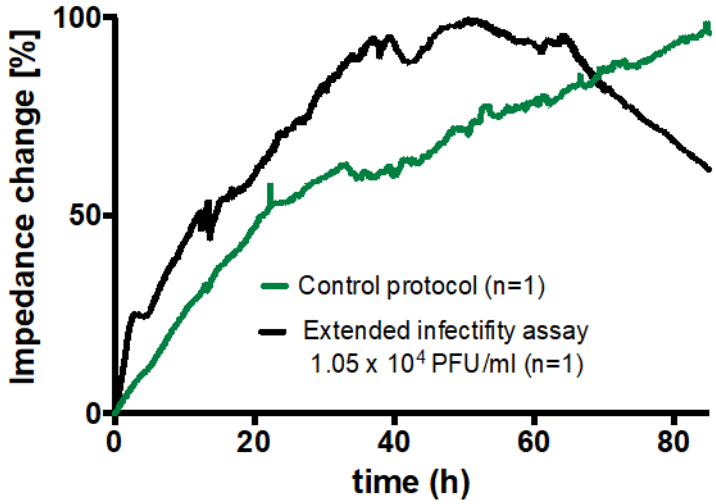

Figure 18: Assay performance evaluation – virus titre 1.05 x 10^4 PFU/ml: Control PG-4 culture (green) compared to the impedance trace of a PG-4 culture with upstream *M. dunni* culture infected with 1.05 x 10^4 PFU/ml.

Next, the initial virus titre was lowered to 1.05 x 10^3 PFU/ml (Figure 19 black). The results were again compared to the control culture (green). Interestingly, the typical decrease in impedance signal upon infection of the PG-4 culture was observed 65 hours into the assay time, however in a second experiment this result could not be confirmed

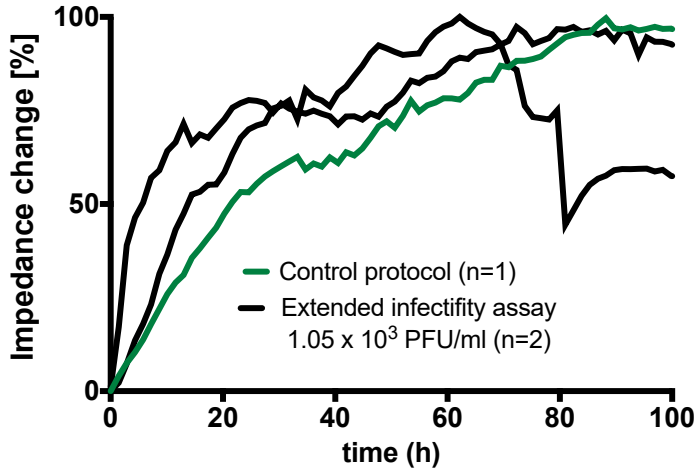

Figure 19: Assay performance evaluation – virus titre 1.05 x 10^3 PFU/ml: Control PG-4 culture (green) compared to the impedance trace of a PG-4 culture with upstream *M. dunni* culture infected with 1.05 x 10^3 PFU/ml.

7 A microfluidic impedance-based extended infectivity assay: combining retroviral amplification and cytopathic effect monitoring on a single lab-on-a-chip platform

7.1 Contribution Statement

Type: published Lab on a Chip, 2021,21, 1364-1372 (2021)

Authors: Michaela Purtscher, Mario Rothbauer, Sebastian Rudi Adam Kratz, Andrew Bailey, Peter Lieberzeit and Peter Ertl

Contributions: Study conception and design: Michaela Purtscher, Mario Rothbauer, Peter Lieberzeit and Peter Ertl; data collection: Michaela Purtscher, Mario Rothbauer and Sebastian Rudi Adam Kratz; analysis and interpretation of results: Michaela Purtscher, Mario Rothbauer, Sebastian Rudi Adam Kratz, Andrew Bailey, Peter Ertl; draft manuscript preparation: Michaela Purtscher, Mario Rothbauer, Andrew Bailey, Peter Ertl, Peter Lieberzeit; All authors reviewed the results and approved the final version of the manuscript.

Lab on a Chip

ROYAL SOCIETY OF CHEMISTRY

PAPER

View Article Online
View Journal

Cite this: DOI: 10.1039/d0lc01056a

A microfluidic impedance-based extended infectivity assay: combining retroviral amplification and cytopathic effect monitoring on a single lab-on-a-chip platform†

Michaela Purtscher,‡[a] Mario Rothbauer, ‡[b] Sebastian Rudi Adam Kratz, [bc] Andrew Bailey,[d] Peter Lieberzeit [e] and Peter Ertl *[b]

Received 21st October 2020,
Accepted 31st January 2021

DOI: 10.1039/d0lc01056a

rsc.li/loc

Detection, quantification and monitoring of virus – host cell interactions are of great importance when evaluating the safety of pharmaceutical products. With the wide usage of viral based vector systems in combination with mammalian cell lines for the production of biopharmaceuticals, the presence of replication competent viral particles needs to be avoided and potential hazards carefully assessed. Consequently, regulatory agencies recommend viral clearance studies using plaque assays or $TCID_{50}$ assays to evaluate the efficiency of the production process in removing viruses. While plaque assays provide reliable information on the presence of viral contaminations, they are still tedious to perform and can take up to two weeks to finish. To overcome some of these limitations, we have automated, miniaturized and integrated the dual cell culture bioassay into a common lab-on-a-chip platform containing embedded electrical sensor arrays to enrich and detect infectious viruses. Results of our microfluidic single step assay show that a significant reduction in assay time down to 3 to 4 days can be achieved using simultaneous cell-based viral amplification, release and detection of cytopathic effects in a target cell line. We further demonstrate the enhancing effect of continuous fluid flow on infection of PG-4 reporter cells by newly formed and highly active virions by *M. dunni* cells, thus pointing to the importance of physical relevant viral–cell interactions.

1. Introduction

In light of current and reoccurring viral outbreaks such as Ebola, Influenza, Zika and most recently SARS-Cov-2, improved detection systems capable of detecting ultralow levels of virus concentrations are of growing interest to the public and the medical community. Additionally, new methods that allow monitoring of virus–cell interactions are equally of importance in the development of virotherapy options, where either native or engineered viruses are used as alternatives in cancer therapies, immunotherapies and delivery vehicles in gene therapy applications.[1,2] Furthermore, reliable and accurate identification of viral contaminations in pharmaceutical products constitutes an essential risk assessment strategy to evaluate the safety of drugs, to date. This safety issue has arisen with the widespread usage of mammalian cell lines in the production of biopharmaceuticals, which potentially can express and release endogenous derived retroviral-like particles. Viral clearance studies are therefore recommended by the Food and Drug Administration (FDA) to evaluate pharmaceutical purification processes.[3] In virus clearance studies the biosafety of pharmaceutical products is determined by (a) selecting the most appropriate virus for the study and (b) assessing process steps that are effective in removing viruses. Among others, the murine leukemia virus as one of the best studied retrovirus is predominantly used in virus clearance studies.[4,5] This virus can be readily propagated without adverse effects in the skin fibroblast cell line *M. dunni* (*mus terricolour*) resulting in the release of large quantities of infectious virus particles, which can be subsequently detected using focus forming and plaque assays.[6,7] This means that in theory the

[a] *University of Applied Sciences FH Technikum Wien, Höchstädtplatz 6, 1200 Vienna, Austria*
[b] *Faculty of Technical Chemistry, Vienna University of Technology (TUW), Getreidemarkt 9, 1060 Vienna, Austria. E-mail: peter.ertl@tuwien.ac.at*
[c] *Institute of Pharmaceutical Technology and Buchmann Institute for Life Sciences, Goethe University, mAx-von-Laue-Straße 15, 60438 Frankfurt am Main, Germany*
[d] *ViruSure GmbH, Donau-City-Straße 1, 1220 Vienna, Austria*
[e] *Department of Physical Chemistry, University of Vienna, Währingerstrasse 42, 1090 Vienna, Austria*
† Electronic supplementary information (ESI) available. See DOI: 10.1039/d0lc01056a
‡ These authors contributed equally.

presence of a single replication competent retrovirus can be detected in pharmaceutical products using a cell-based virus amplification strategy. In contrast to PCR-based strategies that are used as golden standard for quantification of viral content, focus forming assays are based on immunofluorescent labelling of antibodies detecting cytopathic effects of a viral titer on cells. In addition, plaque assays rely on infecting a secondary cell culture (reporter cell line) that in turn forms visual circular cell-free areas and are the golden standard to analyze virus infectiousness or replication.[8,9] Here, the cat brain Moloney sarcoma virus-transformed PG-4 cell line is often used in viral clearance studies for detection of replication competent retroviruses in products and reagents for human use. Although proven effective and recommended by the FDA, the standard assay protocol is labor intensive involves multiple manual steps, is expensive due to the large volumes of cell culture media, reagents and consumables needed and can take up to two weeks to complete using trained biomedical analysts. As an example, a standard assay protocol involves initial virus amplification using *M. dunni* cell cultures, repeated collection of the supernatant, followed by preparation of several dilutions of the virus containing reagent and its addition to a semi-confluent grown PG-4 cell layers usually followed by the coverage with a solid or semisolid overlay to hinder the spread of the virus ad random. Once infected PG-4 cells undergo distinct morphological changes (*e.g.* rounding up and cell detachment) resulting in the formation of cell free areas during the process of viral release, which overtime leads to the formation of visible plaques in the cell layer. To enhance the contrast between cell layer and plaques, a potential cancerogenic and environmentally toxic staining procedure of the cell layer is usually performed at the end of the cultivation period (*e.g.* 9 days) and the number of plaque forming units (PFU ml^{-1}) are microscopically analyzed and calculated in relation to serial dilutions.[10,11]

To overcome some of the limitations associated with detecting virus–host cell interactions a variety of advanced cell-based technologies have been reported to improve automation, miniaturization and integration of biosensing strategies to eliminate tedious staining and endpoint detection. For instance, impedance measurements have been employed to determine viral titers by tracing cytopathic effects induced changes in cell cultures using the commercial available xCELLigence™ real-time cell analysis system (Agilent, USA) and ECIS™ systems (Applied BioPhysics Inc., Germany).[12–14] Despite these efforts to improve outcomes, reduce time-to-result and costs, the complexity of the multistep cell-based assay prevails. As complementary technology to analyze virus–cell interactions microfluidic cell culture systems have been used to detect cell-to-cell, cell-to-matrix and cell-to-surface as well as material–biology interactions especially regarding biocompatibility and toxicology.[15–17] Microfluidic cell culture systems are ideally suited to monitor cytopathic and cytolytic effects of viruses, since laminar flow enables improved particle–cell interactions with high spatiotemporal resolution creating a more controllable and precise microenvironment.[18,19] In the current work we introduce an automated microfluidic-based extended infectivity assay where virus amplification and continuous release of newly formed virions by a primary producer cell line as well as the secondary cytopathic or cytolytic effect on an indicator cell line are monitored on a single lab-on-a-chip platform with non-invasive and dynamic monitoring using embedded impedance microsensors. Rapid detection of replication competent viral particles in samples is readily accomplished with our platform by initially increasing the viral load using the virus replication supporting *M. dunni* cell line, followed by infection of the indicator cell line PG-4 by the newly formed and active virions resulting in a loss of cell-surface integrity (onset of plaque formation). As visualized in Fig. 1 our platform combines the basic virus – host mechanisms in a dual compartment sensing system with an automated microfluidic assay principle to significantly cut down the assay timeline and automate tedious assay steps. An important aspect of our microfluidics approach is the application of constant fluid flow of 1.5 µl min^{-1} during virus uptake, amplification and release resulting in newly formed and active virions that readily infect the downstream PG-4 target cell line,[20] where cell-surface detachment processes are readily investigated by cell impedance sensing.[21,22] Our "Sample In Result Out" microfluidic infectivity assay reduces assay steps by (i) performing dual cell culture handling in parallel, (ii) eliminating supernatant collection and biased sample transfer by manual pipetting, (iii) maintaining higher numbers of replication competent virions and (iv) omitting staining procedures and end-point detection by read-out automation. Our automated microfluidic infectivity assay therefore provides results within a fewer time window and has the potential to reduce costs of QC measures based on standard microtiter plate-based plaque assays when integrated into existing biopharmaceutical work flows.

2. Materials and methods

Chip design and fabrication

The bottom of our lab-on-the-chip device consisted of a (30 × 30) mm^2 borosilicate glass substrate (Schott Borofloat® D263Teco) containing interdigitated electrode structures (µIDES), 200 fingers with electrode finger width as well as a gap distance of 5 µm (1 : 1 ratio) and an IDES area of 2 mm^2 (see ESI† Fig. S1). The fluidic layer consists of polydimethylsiloxane (Sylgard 184) consisting of 100 µm high and wide channels that connect both cell culture chambers. The culture chambers were 20 mm long and 5 mm wide featuring a cell culture area of 95 mm^2 for each chamber. The microfluidic PDMS is layered between the bottom glass substrate containing the microelectrode arrays and a top object glass (VWR international) substrate containing 1 mm in diameter access holes to connect to external tubing. Final assembly of the two glass and PDMS layers were performed

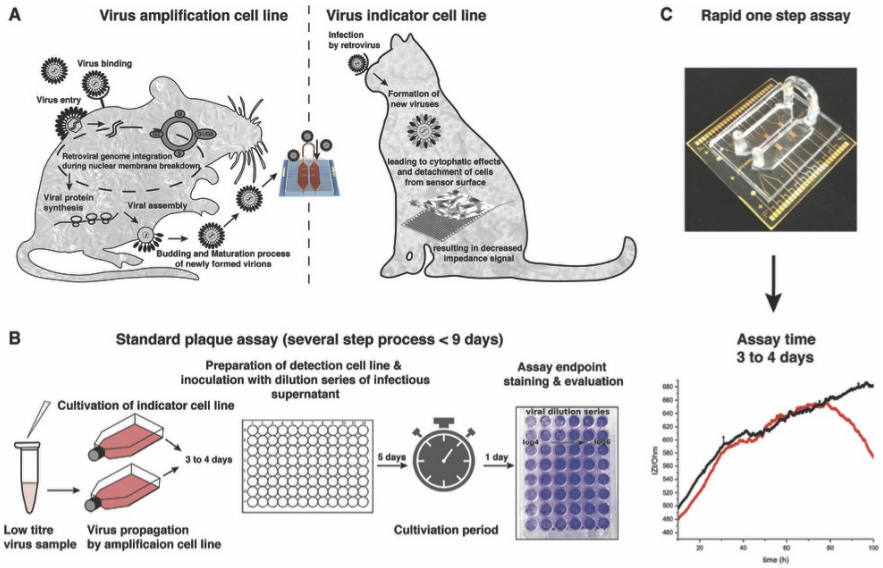

Fig. 1 A.) Schematic overview of the biological principles underlying the proposed extended infectivity assay. Left mouse silhouette indicates the *M. dunni* amplification cell line, that allows for non-cytopathic virus propagation. Middle shows the lab-on-a-chip platform for simultaneous dual cell cultures with embedded impedance sensors. Right cat silhouette indicates the PG-4 indicator cell line which upon superinfection with the model virus shows cytopathic effects and cells detach from sensor surface. B.) Representative outline of the process steps involved in a standard plaque assay protocol. C.) Rapid one step "sample in result out" microfluidic extended infectivity assay based on *M. dunni* cell-based x-MuLV virus amplification and release followed by infection of target PG-4 cells and detection of cytopathic effects using embedded impedance sensors.

by thoroughly cleaning each single substrate followed by plasma activation and bonding.

Bioimpedance spectroscopy

The dual-cell chip was placed onto an aluminium holder and heated to 37 °C, while contact pads located at the sensor substrate were connected *via* spring-laded pins and insulated wires to a VMP3 multi-channel potentiostat (BioLogic). Impedance spectra ranging from 400 Hz to 400 kHz were continuously recorded every 5 min (V peak to peak 140 mV) over a period of 3 to 5 days. For data analysis EC Lab software, Graph Prism 7.0a and OriginPro 8.5 and FlowJo10.3; Dean–Jett–Fox analysis was used. Impedance data were normalized according to ((IZI total column − IZI medium)/(IZI peak − IZI medium)).

Cell culture handling

The cat brain Moloney sarcoma virus – transformed PG-4 cell line (European Collection of Cell Cultures, 94102703) and the normal mouse tail fibroblast *M. dunni* (Clone III8C) cell line (European Collection of Cell Culture, 94101211) were cultured at 37 °C in 5% CO_2 humidified atmosphere (incubator; HeraCell). Cell expansion took place in 25 cm^2 cell culture flaks (PAA Laboratories), where after reaching 70 to 80% confluence both cell lines were split at a ratio of 1 : 6 using 0.25% trypsin–EDTA (trypsin–ethylenediaminetetraacetic acid, fisher scientific) at 37 °C for 3 min for enzymatic cell detachment. The culture medium, McCoys (PAA Laboratories), was supplemented with 1% stabile L-glutamine (PAA Laboratories) and 5% FCS (PAA Laboratories) for the *M. dunni* cell line as well as 10% FCS for die PG-4 cell line. For on-chip experiments cells were transferred into a 6-well plate 24 h prior to their seeding into the microfluidic device at a density of approximately 70% to ensure comparability of the cellular state between experiments. The final cell culture medium was prepared with 10% FCS and complemented with 15 mM HEPES puffer (PAA Laboratories) for on-chip experiments.

On-chip cultivation – extended infectivity protocol

The retrovirus x-MuLV (ATCC®Vr-1447™) strain pNFS Th-1 was obtained from ViruSure GmbH (AT) and stored at −80 °C prior to usage. Prior to cell seeding, the microfluidic device was rinsed for a minimum of 1 h with 70% ethanol followed

by a second rinsing step with PBS supplemented with 1% gentamycin for several hours to ensure sterility. This was followed by flushing the biochip with cell culture medium using a 10 mL gas-tight syringe at 15 μl min^{-1} using a pressure driven syringe pump (Nemesis) for several hours. Next, the flow was set to 1.5 μl min^{-1} and impedance baseline *signals* were recorded as described above. *M. dunni* and PG-4 cells were individually seeded into each cell chamber to cover 40% (6.6×10^4 *M. dunni* cells) and 20% (1.32×10^5 PG-4 cells per 195 μl volume) of the 95 mm^2 cell culture area, respectively. After 2 h of attachment time under static conditions, the culture medium flow rate was set to 1.5 μl min^{-1} and infection of the *M. dunni* cells with varying virus titres was performed after 13.5 h using 1 mL plastic syringe.

Flow cytometry – Cell cycle analysis

M. dunni and PG-4 cells were seeded 24 h prior to the experiment into 6-well plates at an approximate density of 70%. For the experiment itself, both cell types where seeded into 12-well plates at a density of 20% complying to 1.05×10^5 cell per well. Both cell types were cultured under non-starvation, starvation and starvation-release conditions and samples were taken after 24, 48 and 72 h after seeding. After aspiration and rinsing with PBS, cells were detached using 300 μl of a trypsin–EDTA solution and 3 min of incubation at 37 °C. The cells were than resuspended in 1 mL culture medium and centrifuged for 5 min at an acceleration force of 170 g. The supernatant was discarded, and the cell pellet was resuspended in a 2% paraformaldehyde solution (PFA) for 10 min at room temperature. Samples were once more centrifuged for 5 min at an acceleration force of 170 g, the PFA solution was removed, the cells were resuspended in 1 mL blocking buffer (PBS + 0.2% BSA) and stored at 4 °C. Prior to the FACS analysis, cells were stained using the DNA binding dye DAPI. Cells were centrifuged for 5 min at 170 g and cells were resuspended in staining solution comprised of PBS with 0.2% BSA, 0.2% TritionX-100, 100 μg mL^{-1} RNAse and 2 ng mL^{-1} DAPI dilution and kept for 20 min in the dark before analysing *via* FACS.

qPCR – virus sample preparation

Starting after the cell seeding on-chip, at an initial density of 40% confluence, the supernatant of the cell culture was periodically collected and stored at −80 °C. The cell culture was inoculated with a virus titer of 7.7×10^3 PFU ml^{-1} 12 h following cell seeding and supernatants were collected after 6, 12, 24, 30, 36, 42, 48 and 60 h after virus inoculation. The frozen samples were shipped to ViruSure Inc. for qPCR analysis. RNA isolation and reverse transcription was performed according to standard protocols. The qPCR protocol was performed using the Applied Biosystems 7500 real-time PCR System with the following program. Reverse transcription for 15 min at 48 °C, enzyme activation for 10 min at 95 °C followed by 40 cycles of a denaturation phase of 15 s at 95 °C and annealing/extension phase of 1 min at 60 °C.

Computational fluid dynamics – fluid modeling

The CFD simulation was performed by CFD Autodesk 2019. The CAD model of the chip was created in Fusion 360 (Autodesk). The fluid was modeled as water at room temperature. Furthermore, there was no heat exchange and gravity simulated. The fluid inlets were modeled by a defined 1.5 μl min^{-1} of volume flow. The outlets were modeled as openings with 0 pascal pressure (please see table). No further initial conditions were added, and the net was generated automatically by the software.

3. Results and discussion

3.1. Characterization of microfluidic device

Initial microdevice characterization was performed using computational fluid dynamics (CFD) simulation and fluorescent imaging of labelled nanoparticles (diameter of 100 nm) within the two-chamber lab-on-a-chip system to analyse viral transport behaviour. Results shown in Fig. 2A revealed identical measurement conditions for both cell culture chambers, while nanoparticle movement from the upstream-located virial amplification cell culture chamber to the viral detection cell chamber required 20 min in the presence of 1.5 μl min^{-1} fluid flow. Therefore, it takes approx. 10 min for the nanoparticles to pass over sensor region 1 and 2 within a single chamber (see Fig. 2B), thereby ensuring sufficient time for virus to cell interactions.

Next, biosensor sensitivity, cell adhesion and growth curve dynamics of *M. dunni* and PG4 cell lines was assessed using the on-chip electrochemical impedance measurements. Since sensitivity of an cell-based impedance assays is influenced by sensor geometry, frequency analyses for both cell types were conducted.[23,24] Fig. 3A shows impedance spectra of confluent cell monolayers of *M. dunni* and PG-4 using the 5 × 5 μm gap-to-finger geometry. To verify that no significant signal maxima shifts are present due to cell line differences, frequency analyses were performed using infected *M. dunni* and PG-4 cells. Results shown in ESI† Fig. S2 point at similar frequency dependent sensor sensitivities of *M. dunni* (n = 11) and PG-4 (n = 10) cultures, which were infected by increasing titres of the x-MuLV prior measurements.

Interestingly the lower impedance signal change-fold observed with infected PG-4 cells (indicator cell line) already indicates the occurrence of cytopathic effects of the retrovirus resulting in cell detachment and cell lyses. In a next set of experiments, cell attachment, spreading and proliferation of *M. dunni* cells (amplification cell line) were investigated to characterize on-chip growth behaviour of healthy cells. It is important to note that *M. dunni* cells need to be seeded at a low surface coverage of max. 40% to allow cells to proliferate and thereby undergo all cell cycle phases (G1, S, G2 and M). This is crucial to ensure effective integration and amplification of the retroviral genome into the proliferating

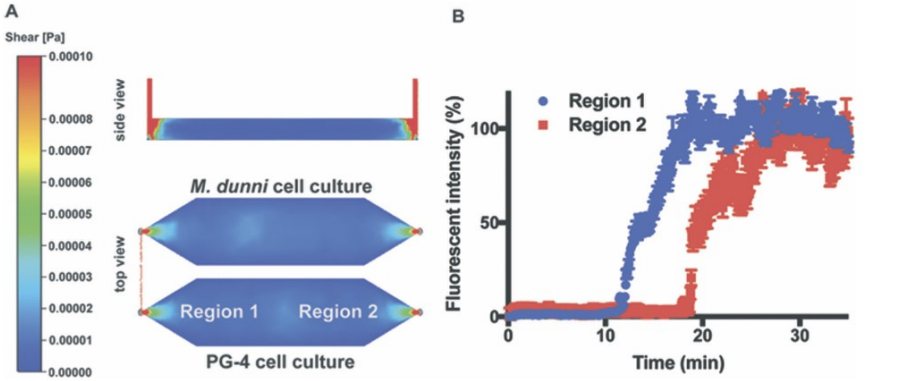

Fig. 2 A.) Distribution and shear stress analysis by CFD simulation of the two-chamber lab-on-a-chip system. Flow velocity in both culture chambers show similar profiles with a higher shear stress levels in the area of ports and connectors while a fluid flow of 1.5 µl min^{-1} was applied. B.) Tracing of fluorescence labelled nanoparticle with a diameter of 100 nm over the area of (upstream) region 1 to region 2 (downstream) within a single cell culture chamber. Nanoparticle remain approximately 20 min within one culture chamber before passing over to the second chamber.

M. dunni cell line. Impedance-time traces shown in Fig. 3B reveal a rapid signal increase within the first 4 h (*e.g.* cell attachment) after cell seeding followed by a slow signal decrease (*e.g.* cell spreading) of (1.55 ± 0.77) *Ohm* h^{-1} (n = 12) for 25 h resulting in stable impedance signals between 40 to 45 h, which indicates the establishment of fully covered sensor surfaces and stable cell layers up to 100 h of cultivation duration. ESI† Fig. S3A depicts the representative change in sensor coverage during impedance sensing of *M. dunni* cells over the whole culture period. Similarly, the establishment and stability of PG-4 indicator cell line over a period 100 h cultivation inside the microfluidic biochip was confirmed using the embedded impedance sensors. Fig. 3C shows a steady signal increase of in average (1.04 ± 0.62) *Ohm* h^{-1} (n = 9) over the first 65 h after which a plateau is reached that indicates sensor coverage by PG-cells (ESI† Fig. S3B). The fact that the chip-based PG-4 cell culture reaches confluency approximately a day later than *M. dunni* cells is ideally suited to perform dual cell cultivations in parallel to the infectivity assay, thus eliminating multiple cell-loading steps at different time points. It is of importance that the cell-based virus-amplification carried out by *M. dunni* cells takes place prior to reaching a confluent PG-4 monolayer to ensure effective integration of the retroviral genome and manifestation of its cytopathic effects.

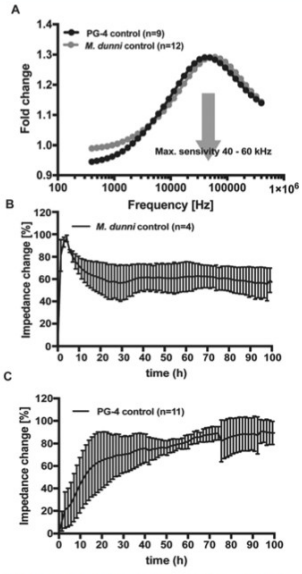

Fig. 3 Sensor sensitivity, cell adhesion and growth curve dynamics of the integrated impedance sensors: A) analysis of frequency dependent sensor sensitivity of PG-4 (n = 9) and *M. dunni* (n = 12) control cultures. B and C), Growth curve dynamics of *M. dunni* (n = 4) and PG-4 (n = 11) control culture over the time course of 100 h.

3.2. Cell-based virus amplification and infection efficiency

A key aspect of any viral infectivity assay is the successful integration of retroviral DNA into the host genome, which takes place during cell mitosis in particular during the nuclear membrane breakdown. The production of x-MuLV viral progeny usually begins within 18 h to 24 h after infection (see also ESI† Fig. S4), which makes a time-oriented infection protocol an important issue in optimizing the on-chip co-cultivation protocol. Since mammalian cell mitosis

last only for about 2 h, cell cycle synchronization of the entire cell culture may improve infection rates by increasing the number of cells present in the G2/M phase at the time of infection. To assess the impact of a 48 h pre-starvation period as a simple drug-free means to induce cell cycle arrest, on-chip cell culture phase synchronisation was analyzed using time-resolved FACS analyses. Fig. 4 shows cell cycle distributions over time in the absence and presence of starvation as well as "release of starvation" using both *M. dunni* and PG-4 cells. In the absence of cell starvation, *M. dunni* cell cycle distribution over a 72 h period grown in full media revealed that a majority of cells (>60%) within the cell population resides in the G1 phase, while a significant increase in G2/M phase occurred only after 13–17 h and 26 h, respectively (see Fig. 4A). This phenomenon can most likely be attributed to cells re-entering a proliferative state after a delay in cell cycle progression due to initial attachment and spreading events within the first 10 h. As a result, an increase of cells in G2/M phase up to 33% of the total cell population 13 h after cell seeding is repeatedly obtained. Interestingly, G2/M phase population remained stable over the next 17 h of cultivation, indicating that under regular growth conditions, virus addition is optimally performed at about 13 h of *M. dunni* on-chip cultivation. A direct comparison of cell cycle distribution using complete growth medium, serum depleted medium and release out of a 48 h starvation period is shown in Fig. 4B. Interestingly neither starvation using serum free medium nor release out of starvation after a 48 h pre-starvation period increased the amount of cells residing in the G2/M phase, which is reflected also by an average cell doubling time of 14.7 to 16.7 h of *M. dunni* cells. Since cell cycle synchronization did not yield any advantage over our regular cell culture protocol, virus addition was set at 13.5 h post cell ceding to ensure efficient integration of host cell genome in all subsequent on-chip experiments. These findings are further supported by time-resolved qPCR analyses, where the release of newly formed virions by *M. dunni* cells 12 h after infection with a x-MuLV titer of 7.7×10^3 PFU ml^{-1} was quantified. Results shown in ESI† Fig. S3 confirm constant virus propagation over time exhibiting a linear increase over 66 h in culture. Additional FACS results shown in Fig. 4C highlight that PG-4 cells are ideally suited to serve as indicator cell line for x-MuLV infection studies, since over 50% of the cell culture displays a G2/M phase at any given timepoint. In order words, PG-4 cells can be readily infected by freshly produced virus particles over the entire analysis period of our on-chip infectivity assay.

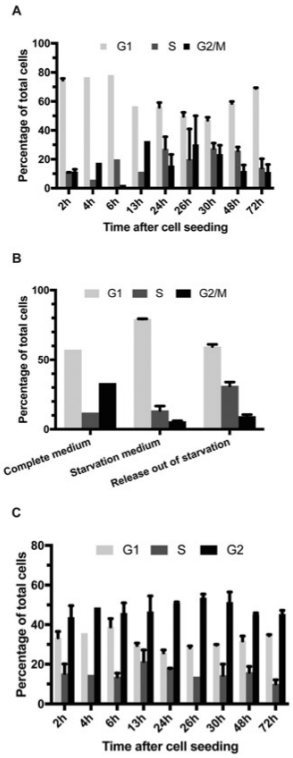

Fig. 4 Drug-free and starvation-induced cell cycle synchronisation analysis using FACS: A) *M. dunni* cells cultured in complete growth medium. B) Comparison of cell cycle populations of *M. dunni* cultures 13 h after cell seeding of cultures in complete growth medium as well as cultures starved by serum depletion and cultures 12 h after release from a 48 h starvation period. C) PG-4 cell cultures in complete growth medium.

3.3. Application of the microfluidic sensor-integrated system as extended infectivity assay

Prior to the application of the extended infectivity assay, impedance signals in the presence of infected *M. dunni* cell cultures were investigated to determine possible viral induced side effects such as loss of sensor signals as a result of cell detachment processes. Fig. 5A shows impedance time-traces of healthy and *M. dunni* cells inoculated with a virus titer of 7.7×10^3 PFU ml^{-1}, translating to 1.5×10^3 PFU per culture chamber. Although signal differences were observed for the first 4 h of cultivation, stable impedance-time traces are obtained for healthy and infected *M. dunni* cells for the remaining 96 h of on-chip cultivation. Interestingly, obtained impedance signals are in average by 2-fold higher in the presence of infected cells that constantly release newly formed virions as seen in Fig. 5B. However, regardless of infection status impedance signals reached a plateau already after 30 h in on-chip cultures (see Fig. 5A). Moreover, a successful infection of *M. dunni* cells, the amplification cell line, can also be recognized by an increase of impedance values.

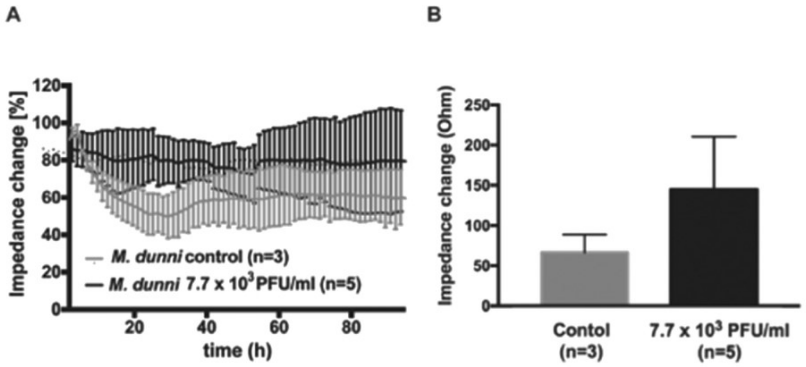

Fig. 5 A) Comparison of *M. dunni* impedance time traces of single *versus* dual cell cultures. While the grey (n = 3) trace show *M. dunni* control cultures the black (n = 5) one show *M. dunni* coupled to PG-4 cultures which were additionally infected at a titer of 2.2×10^5 PFU ml^{-1}. B) Absolute impedance changes (*Ohm*) over the culture period of 90 h.

When finally coupling *M. dunni* cell cultures to the PG-4 indicator cell line similar growth dynamics (data not shown) are observed, indicating that reproducible co-culturing in parallel is feasible in the current microfluidic dual-cell chip system. To rule out any influence of the *M. dunni* culture upstream of the PG-4 reporter cell line, impedance curves of PG-4 in co-culture with *M. dunni* cells from the extended infectivity assay was compared with PG-4 monocultures (n = 11) with no discernable difference observable (see ESI† Fig. S7). In a next set of experiments, the ability of the microfluidic extended infectivity assay to rapidly detect cytopathic effects induced by virions in PG-4 indicator cells that were produced by the upstream located *M. dunni* cells is evaluated. Following individual loading of each cell culture compartments (*e.g.* 40% *M. dunni* and 20% PG-4) intended to prevent cell cross contaminations, the cell cultivation chambers were manually connected and a flow rate of 1.5 µl min^{-1} was adjusted, and impedance measurements were conducted over the entire assay period of 100 h. As shown in Fig. 6A the microfluidic extended infectivity assay containing embedded electrical microsensors already detected the onset of virus-induced cytopathic effects such as cell rounding and detachment of PG-4 cells after only 60 h (<3 days) in cultivation resulting in impedance decrease. Here, *M. dunni* cells were infected with x-MuLV at a concentration 2.2×10^5 PFU per culture chamber, which was more than sufficient to induce cell-based virus amplification and release. Final performance evaluation involved the effectiveness of the extended infectivity protocol using our dual cell chip set up over a single cell culture system. Results in Fig. 6b show obtained signal fold changes between 60 to 100 h of assay time. The 2.45 ± 0.69-fold signal decrease using the extended infectivity assay strongly points at increased PG-4 cell rounding, detachment and death rates following infection with newly formed virions by *M. dunni* cells. Interestingly, in the absence of *M. dunni* cell where PG-4 cells were directly infected with viral stock solutions at seeding (t = 0) or 13.5 h after seeding a significant difference were observed, thus highlighting the amplification effect of using a dual cell culture set up.

Impedance-time traces (grey line) in control experiments showed typical growth curves and stable cell monolayer integrity of healthy PG-4 cells exhibiting a steady signal increase over time. Importantly, ESI† Fig. S5A shows best

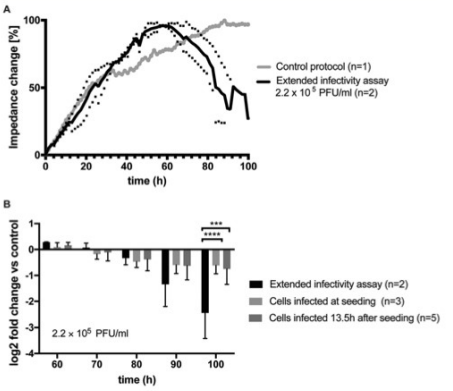

Fig. 6 A) Impedance time trace of PG-4 cell cultures infected with 2.2×10^5 PFU ml^{-1} using the extended infectivity assay protocol (black, n = 2) in comparison to untreated control (grey, n = 1). B) Comparison of fold changes in impedance signal to control using different infection protocols. A −2.45 ± 0.69 fold change in impedance signals was observed after 100 h of assay time in the presence of the extended infectivity assay protocol. Also, significant differences to directly infected PG-4 cultures without in-line amplification through connected *M. dunni* cultures was evident (2-way ANOVA, Turkey's multiple comparison test, p = 0.0001 (***), p < 0.0001 (****)).

performance were obtained using the single-step co-culture system, further highlighting the importance of a timed assay protocol. In turn, ESI† Fig. S5B shows impedance-time traces of directly infected PG-4 cells using a 2.2×10^5 PFU ml^{-1} viral titer added after cell seeding and 13.5 h of culture, respectively. Results of this timed infection study revealed that cytopathic effects in PG-4 cell can be readily detected using impedance measurements, however obtained average signal decreases of 30% between 60 h to 70 h is less dominant than seen using a cell-based virus amplification strategy. This demonstrates that in the presence of similar viral titers, the directly produced and newly formed viruses in our co-culture system are highly potent, active and infectious. In a final control experiment, the microfluidic extended infectivity assay was exposed to heat inactivated x-MuLV titers to confirm that only replication-competent virus particles are detected in the dual-cell chip system. Impedance-time trace seen in ESI† Fig. S6 also shows a steady impedance signal increase reaching a plateau after 70 h, thus pointing at normal growth characteristics for the first three days followed by a rapid loss of impedance as a result of cytopathic events. The brief signal recovery at 80 h can be linked to fluid flow disruption during changing of the media supply syringe at the external pumping station. In summary, our results clearly demonstrate the potential benefits of downscaling, miniaturizing and integrating cell culture systems, since our microfluidic extended infectivity assay coupled with impedance sensors is able to provide results in less than 4 days instead of over one to two weeks required when using the standard plaque assay protocol.

4. Conclusion

The main principle of our microfluidic extended infectivity assay is based on the on-chip combination of cell-based viral amplification using *M. dunni* cells and detection of cytopathic effects of newly formed and highly active virions in target PG-4 cells using embedded impedance sensors. Only the application of an advanced microfluidic cell-based assays will eliminate multiple sequential cell culture handling steps and staining procedures needed for microscopic readouts. While simultaneous co-cultivation of both cell lines in a common lab-on-a-chip systems eliminates numerous and tedious cell culture handling steps, the inherent sensitivity of the bioimpedance sensors allows the time-resolved assessment of cytopathic effects such cell rounding and detachment events as of infected PG-4 cells. We have shown that time-to-result in viral clearance studies can be significantly reduced from over a week down to 4 days, using a simple cell culture and infection protocol. Another benefit of using a dynamic cell assay protocol is that new formed virions are actively transported to the indicator cell line, thus ensuring constant and effective virus – cell interactions.

Despite the advantages of using an improved microfluidic dual cell culture system over standard plaque assays, some limitations still remain and are associated with its industrial integration. Key for a successful implementation for viral clearance studies is concerned with assay parallelization and increased throughput. In particular additional automation to generate virus titrations, perform sample and cell loading procedures as well as dose–response analysis routines still need to be integrated to ensure reliable adaptation into pharmaceutical safety evaluations and quality control measures. However, automation and parallelization can also be accomplished by increasing the numbers of cultivation chambers and integrating additional microfluidics components such concentration gradients and mixers. Also, replacement of the active flow control using external syringe pumps with passive flow strategies (*e.g.* refilling of reservoirs) may allow the application of robotic pipetting stations leading to improved sample throughput, thus presenting a real alternative to plague assays.

In summary, the developed microfluidic extended infectivity assay has shown to provide reliable results even when using low to medium viral titers. However, it is not entirely clear whether ultralow concentrations of replication-competent particles present in a final pharmaceutical product can be detected within a limited assay time of 4 days. A comparative analysis within an industrial QM setting is still needed to fully evaluate the potential of our microfluidic extended infectivity assay for viral safety evaluation in pharmaceutical production. Since a direct performance evaluation and benchmarking against standard plaque assays also requires a significant adaptation in biochip layout to deal with the increased sample volume, it is, however, beyond the current study and subject to future development.

Conflicts of interest

There are no conflicts to declare.

Acknowledgements

We thank Dipl.Ing. Natascha Hodosi for her technical support with the performance of qPCR experiments. The authors gratefully acknowledge the financial support from the Austrian Research Promotion Agency (FFG: # 815477/13900) and ViruSure GmbH (Vienna, Austria).

Notes and references

1 E. Ylösmäki and V. Cerullo, *Curr. Opin. Biotechnol.*, 2020, **65**, 25–36.
2 N. Slade, *Period. Biol.*, 2001, **103**, 139–143.
3 FDA (Food and Drug Administration), Fda, 2020, 16.
4 A. Rein, *Adv. Virol.*, 2011, **2011**, 403419.
5 J. W. Hartley, N. K. Wolford, L. J. Old and W. P. Rowe, *Proc. Natl. Acad. Sci. U. S. A.*, 1977, **74**, 789–792.
6 P. T. Peebles, *Virology*, 1975, **67**, 288–291.
7 D. K. Haapala, W. G. Robey, S. D. Oroszlan and W. P. Tsai, *J. Virol.*, 1985, **53**, 827–833.
8 R. H. Bassin, S. Ruscetti, I. Ali, D. K. Haapala and A. Rein, *Virology*, 1982, **123**, 139–151.

9 Z. Li, M. Blair and L. Thorner, *J. Virol. Methods*, 1999, **81**, 47–53.
10 A. Baer and K. Kehn-Hall, *J. Visualized Exp.*, 2014, 1–10.
11 M. J. Chiang, M. Pagkaliwangan, S. Lute, G. Bolton, K. Brorson and M. Schofield, *Biotechnol. Bioeng.*, 2019, **116**, 2292–2302.
12 C. Charretier, A. Saulnier, L. Benair, C. Armanet, I. Bassard, S. Daulon, B. Bernigaud, E. Rodrigues de Sousa, C. Gonthier, E. Zorn, E. Vetter, C. Saintpierre, P. Riou and D. Gaillac, *J. Virol. Methods*, 2018, **252**, 57–64.
13 S. Lebourgeois, A. Fraisse, C. Hennechart-Collette, L. Guillier, S. Perelle and S. Martin-Latil, *Front. Cell. Infect. Microbiol.*, 2018, **8**, 335.
14 M. R. Pennington and G. R. Van de Walle, *mSphere*, 2017, **2**, 1–12.
15 J. Rosser, B. Bachmann, C. Jordan, I. Ribitsch, E. Haltmayer, S. Gueltekin, S. Junttila, B. Galik, A. Gyenesei, B. Haddadi, M. Harasek, M. Egerbacher, P. Ertl and F. Jenner, *Mater. Today Bio*, 2019, **4**, 100023.
16 M. Rothbauer, V. Charwat, B. Bachmann, D. Sticker, R. Novak, H. Wanzenböck, R. A. Mathies and P. Ertl, *Lab Chip*, 2019, **19**, 1916–1921.
17 M. Rothbauer, I. Praisler, D. Docter, R. H. Stauber and P. Ertl, *Biosensors*, 2015, **5**, 736–749.
18 G. Birnbaumer, S. Küpcü, C. Jungreuthmayer, L. Richter, K. Vorauer-Uhl, A. Wagner, C. Valenta, U. Sleytr and P. Ertl, *Lab Chip*, 2011, **11**, 2753–2762.
19 H. Zirath, M. Rothbauer, S. Spitz, B. Bachmann, C. Jordan, B. Müller, J. Ehgartner, E. Priglinger, S. Mühleder, H. Redl, W. Holnthoner, M. Harasek, T. Mayr and P. Ertl, *Front. Physiol.*, 2018, **9**, 1–12.
20 J. M. Coffin, S. H. Hughes and H. E. Varmus, *Retroviruses*, 1997.
21 I. Giaever and C. R. Keese, *Nature*, 1993, **366**, 591–592.
22 W. Gu and Y. Zhao, *Expert Rev. Med. Devices*, 2010, **7**, 767–779.
23 N. S. Mazlan, M. M. Ramli, M. M. A. B. Abdullah, D. S. C. Halin, S. S. M. Isa, L. F. A. Talip, N. S. Danial and S. A. Z. Murad, *AIP Conf. Proc.*, 2017, **1885**, 020276.
24 M. L. Gelsinger, L. L. Tupper and D. S. Matteson, *Int. J. Biostat.*, 2020, **16**, 1–12.

Article

Supporting information: A microfluidic impedance-based extended infectivity assay: Combining retroviral amplification and cytopathic effects monitoring on a single lab-on-a-chip platform

Received 00th January 20xx,
Accepted 00th January 20xx

DOI: 10.1039/x0xx00000x

www.rsc.org/

Michaela Purtscher[a,£], Mario Rothbauer[b,£], Sebastian Rudi Adam Kratz[b,c], Andrew Bailey[d], Peter Lieberzeit[e] and Peter Ertl[b,*]

2. Materials and methods

Chip design and fabrication

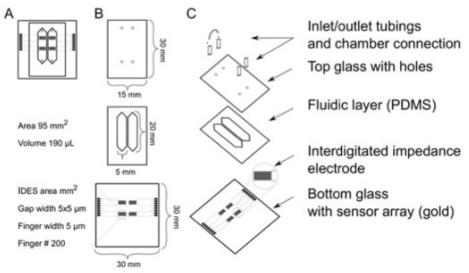

Figure S1: Schematic overview of the Lab-on-a-chip device: A) representation of the specifications of the assembled device. B) Top view on the single layers, including base with embedded sensors, two-chambered fluidic layer for cell cultures and top layer with holes for connective tubing. C) Exploded isometric perspective of the device.

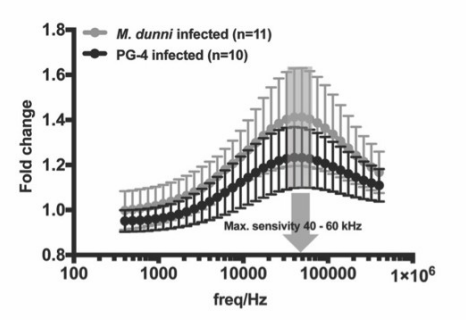

Figure S2: Analysis of frequency dependent sensor sensitivity of and *M. dunni* (n=11) and PG-4 (n=10) cultures infected by various titres of the x-MuLV.

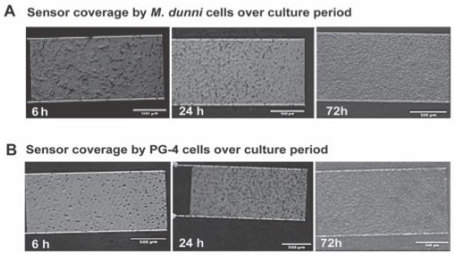

Figure S3: Sensor cell coverage throughout culture period: A.) and B.) Representative images of healthy *M. dunni* and PG-4 cultures at 6, 24 and 72h after cell seeding (scale bar 500 µm).

[a] *University of Applied Sciences FH Technikum Wien, Höchstädtplatz 6, 1200 Vienna, Austria*
[b] *Faculty of Technical Chemistry, Vienna University of Technology (TUW), Getreidemarkt 9, 1060 Vienna, Austria*
[c] *Institute of Pharmaceutical Technology and Buchmann Institute for Life Sciences, Goethe University, mAx-von-Laue-Straße 15, 60438 Frankfurt am Main, Germany*
[d] *ViruSure GmbH, Donau-City-Straße 1,1220 Vienna, Austria*
[e] *Department of Physical Chemistry, University of Vienna, Währingerstrasse 42, 1090 Vienna, Austria*

*corresponding author: peter.ertl@tuwien.ac.at (P.E.)

£ These authors contributed equally

Electronic Supplementary Information (ESI) available: [details of any supplementary information available should be included here]. See DOI: 10.1039/x0xx00000x

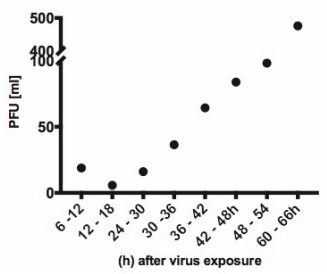

Figure S4: Quantification of PFU/ml in supernatant of *M. dunni* cell cultures inoculated with an initial virus titre of 7.7 × 103 PFU/ml 12 h after cell seeding.

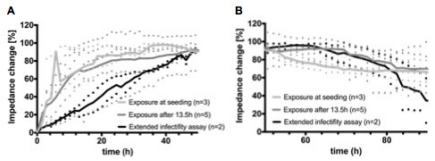

Figure S5: Comparison of impedance traces during assay procedure optimization: A) First 50 h of impedance trace of PG-4 cell cultures exposed with a virus titer of 2.2 × 105 PFU/ml at the time point of cell seeding (light grey), virus exposure after 13.5 h (grey) and coupled in dual culture to the propagation cell line (black). B) Close up of the decreasing impedance signals after the onset of cytopathic effects in the PG-4 cultures. (Exposure at seeding reflect the inoculation with virus supernatant at the beginning of the cell culture period with uncoupled chambers, exposure after 13.5 h the cell cycle dependent timed inoculation with uncoupled cell cultures and finally the established extended infectivity assay protocol.

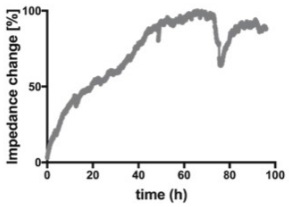

Figure S6: Impedance time trace of PG-4 cells inoculated with a heat inactivated viral supernatant of 2.2 × 10^5 PFU/ml.

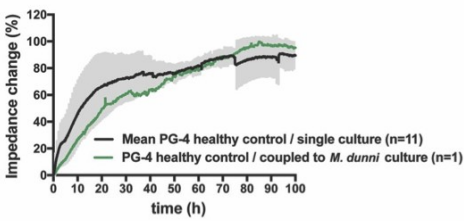

Figure S7: Comparison of growth curve dynamics of PG-4 healthy control coupled to *M. dunni* culture (green) (n=1) to the mean (shaded in grey) of PG-4 healthy control single culture (n=11) over the time course of 100 h shows no significant difference (data set within 1 σ).

8 Discussion and Conclusion

One of the advantages of utilizing impedance sensing methods for the investigation of virus propagation and virus-host interactions is the possibility of monitoring these events in a time-resolved manner. Today's golden standard to investigate viral infections is still the plaque assay. As an end-point assay, information about the onset of infection or viral propagation kinetics are not recorded. Besides, performing plaque assays and similar end-point assays are usually labour intensive. Furthermore, they require high amounts of virus-containing reagents for the establishment of standard curves and the assay itself. Microfluidic technology allows parallelization and automatization and thus reduces the need for high volumes of reagents by orders of magnitudes. The introduction of impedance sensing enables live monitoring of cell cultures, thereby further enhancing microfluidic-based methods for viral detection assays. For example, Lebourgeois *et al.* used the commercially available xCELLigence™ Real-Time Cell Analysis system to detect the Hepatitis A virus to validate the effect of anti-viral treatments [84]. M. Pennington und G.R. Van der Walle employed a system from ECIS Applied BioPhysics to study growth kinetics of the alphaherpesvirus by employing impendence tracing [85]. In the proposed method, the advantages of microfluidic and impedance sensing technologies were combined and extended by co-culturing a virus propagation cell line and a virus detection cell line. Furthermore, additional parameters can be monitored simultaneously; thus, reducing assay time and reducing overall costs. Moreover, the possibility of microscopically inspecting the cell layers at any given time point, the monitoring of the impedance traces of the virus amplifying cells enabling an internal assay quality control. As shown in Figure 16, *M. dunni* cells exhibit a distinct impedance trace when cultured alone and in combination with PG-4 cells. By lowering the temperature, the *M. dunni* cells started to die which can be observed by the strong change in impedance signal. Thus, the progress of the assay can be monitored and interrupted if needed without losing additional time.

The constant flow applied during the assay enables the transportation of the freshly produced virus particles from the *M. dunni* culture chamber over to the PG-4 culture. In addition Zhou *et al.* demonstrated in their work [86] that constant flow enhances the viral spread throughout the cell culture and thus potentially allowing for earlier detectible onset of cytopathic effects by the virus. This is supported by the work of Cimetta *et al.* in which they extensively studied the dynamics of diffusion versus bulk movement of viral particles. The diffusion coefficient was assumed to be 6.0 x 10 - 12 m^2 s^{-1}, based on an approximated hydrodynamic diameter [87], which resembles the virus used in the presented method.

Cells can be infected by more than one virion and therefore also have more than one provirus copy integrated in their genome. Usually the number of integrated proviruses ranges from 2 – 10 copies. At a certain point in time a cell cannot be infected by further virions due to superinfection resistance [55]. Since at a steady state, usually 24 hours to 48 hours after infection, a cell releases only a few 100 physical particles a day which corresponds to only 1 – 10 PFU per day the constant bulk movement of the medium is especially important to shorten the assay time. Thus, even low MOI levels (Multiplicity of infection) should subsequently lead to high infection efficiency levels throughout the cell culture. Another advantage of

the immediate transport to the detection cell line is the avoidance of decreased infectivity potential of the viral particle due to their short half-life time and potentially virus inactivating effects by freeze-thaw cycles, transportation process and similar. Vu *et al.* not only could show a 1.4 to 3.7-fold increase in infective virus particles while employing microfluidic technology but also highlighted the advantage of the constant immediate viral supply for infection of target cells during production and evaluation processes of retroviruses [87].
To enhance the sensitivity of the impendence-based assay the onset of CPE effects needed to be synchronised throughout the cell culture. As a consequence, more cells will detach from the sensor surface at once leading to a sharp decrease in impedance signal indicating the presence of active virus particles. Moreover, this also reduces the chance of the cell layer growing back to confluency before low virus titre induced CPEs can be observed; thus, avoiding long assay times that might prevent conclusive results.
Therefore, of the main objectives of the proposed assay protocol was the optimization of the infection time point with the x-MuLV. This could be achieved by taking the cell cycle of the culture as well as the life cycle of the virus into consideration. In most mammalian cells mitosis lasts for about 2 hours after which they progress into the G1 phase which lasts for approximately 10 hours in actively proliferating cells, followed by the S phase, 5 to 6 hours, and the G2 phase of 3 to 4 hours prior to the next mitosis phase[88]. Meanwhile the intracellular half-life of the virus is set to 5.5 to 7.5 hours [89].
To enrich the population of G2/M phase cycling *M. dunni* cultures, cell cycle synchronization protocols were considered. However, it could be shown that neither serum-starved cell cultures nor cultures which where firstly starved and afterwards kept in full medium led to significant benefits over the synchronization by enzymatical detachment. In fact, in serum-starved cultures lower G1 population levels accompanied by an increase in G2/M and S-phase populations, 13 hours after the start of conditioning
indicate some proliferating cells regardless of the serum depletion. Serum starvation therefore did prove to be potent for cell culture synchronization of *M. dunni* cells, with increasing percentage of G1-phase positive cells towards 72 h. However, an increase in G2/M phase cells could not be observed until 24 hours of cell culture. For cultures which were released from 48 hours long starving period high percentage of S-phase cells at 12 and 22 hours could be identified and indicate a higher fraction of G2/M cells between 12 and 22 hours as well as after 22 hours since this is the following cell cycle step. Since no further samples in this time periods were taken, such conclusions are speculative and although the potential most likely would not balance out the resulting prolongation of the assay time.
However, enzymatical detachment led to sufficient cell population synchronization of cell in G2/M phase 13 hours and 26 after re-seeding in full medium cultures. Aftwards, G1 phase cell population increased and S and G2/M phase populations continually decreased, indicating the culture reaching the confluency and stopped proliferation due to contact inhibition. The second peaking of the G2/M phase population 13 – 17 hours into the culture time further correlates with the average cell doubling time of 14.7 to 16.7 hours of *M. dunni* cells, (data not shown), and presents therefore a second window for re-infecting those cells, leading to higher copy numbers of the virus in any given cell.

Our findings are in accordance with literature which shows that in a proliferating cell culture up to 40 - 60% of all cells are usually in G1 phase at any given moment [90]. It is known that anchorage-dependent cells are temporarily disturbed in their cell cycle progression due to the enzymatically detachment from their growing substrate, resulting in an accumulation of cells in the G1 phase and decrease of cells in S-phase [91]. Studies have further shown, that cells which are in S, G2 or M phase transition throw the cell cycle until the reach the G1 phase, increasing the percentage of cells in G1 phase, already temporarily arrested [89]. This effect permits a semi-synchronization of the cell culture in course of the cell seeding for an on-chip experiment without using any additional treatments, which could alter susceptibility of the virus to the cells.
The optimal time-window to start the infection process was therefore set to 12-13.5 hours prior to the phase at which high percentage of cells would pass through the G2/M phase. This is also consistent with the time needed for the virus to enter the host cell and reach the point at which the integration into the genome can occur.
No adjustments or cell synchronization processes were found necessary for PG-4 cell cultures. Cell cycle analysis revealed that regardless of the cultivation method a constantly high percentage of cells were in G2/M phase at any given time-point, conforming the PG-4 cells as an optimal indicator cell line for retroviral detection methods.
In combination with the cell cycle experiments the propagation of viral particles by *M. dunni* cell cultures were determined using qPCR analysis to ensure sufficient supply for the indicator cell line and confirm the assay protocol. Exposure of the cultures to a virus titre of 2.2×10^5 PFU/ml, 6 hours after cell seeding resulted in the highest numbers (over 10.000 PFU/ml) of fresh virions 72 hours into the assay. Cultures which were exposed to the same virus titre but only 26 hours after seeding showed values of only 7 PFU /ml after 72 hours. This can be explained by the culture starting to reach confluency, with increasingly more cells getting arrested in G1-phase starting 30 hours into the culture time rendering further infections by the virus impossible.
Although a direct comparison of the qPCR results for exposing cell culture either 6 or 12 hours after cell seeding is not feasible since different initial virus titres were used (2.2×10^5 and 7.7×10^3 PFU/ml respectively). The optimal time point for viral exposure was determined to be 13.5 h. This is because the exposure to the virus 6 hours into cell culture lead to high amounts of detectible virus particles. Presumably this would also be true for lower virus titres, however infecting the *M. dunni* cultures that early the PG-4 culture would still be in the adherence and spreading phase (Figure 3C of [21]). This could potentially interfere with the sensitivity of the assay since cytopathic effects would result in lower decrease of the impendence signal and could be attributed to a slow growing cell culture or overlooked completely.
Although it could be shown that the proposed assay can reduce the time to detect cytopathic effects by the x-MuLV down to 3 days, some limitations remain when trying to detect a low initial virus titre. In Figure 17 the impedance trace of a non-infected PG-4 cell culture is compared to the traces cultures infected with 1.05×10^3 and 1.05×10^2 PFU/ml. In this experiment, the PG-4 cultures were directly infected at the time point of seeding without coupling them to *M. dunni* cells and

therefore do not follow the extended infectivity assay protocol. As expected, no clear CPEs could be traced by employing impedance sensing.
When the extended infectivity protocol was applied and the *M. dunni* cells were infected with 1.05 x 10^4 and 1.05 x 10^3 PFU/ml, (Figure 18 and Figure 19). The culture infected with 1.05 x 10^4 PFU/ml showed CPEs around 65 hours into the assay. However, in one of the sets of experiments with an initial virus titre of 1.05 x 10^3 PFU/ml, CPE effects could be observed as well after 65 hours but in a second set this result could not be reproduced. Experiments with lower initial virus titres have to be repeated for further evaluation of the assay robustness and sensitivity. However, various research groups could demonstrate that impedance sensing can be used to detect low virus titres. Charretier *et al.* for example demonstrated the applicability by tracing CPEs of cells from low initial virus titres by employing the xCELLigence™ Real-Time Cell Analysis system [92]. Noteworthy, their experiments were performed over the time frame of more than one week. The here proposed assay was not yet tested over such long periods for lower virus titres since this work was focused on the detection of CPEs within the first 3 to 4 days of viral infection.
However, improvements to lower the detection limit can still be exploited. One opportunity would be to change the surface of the cell culture chambers. It is well known that PDMS does absorb proteins on the surface which than are not available in the cell culture. Xu *et al.* proposed such events influencing their studies at least in the first phase during the culture protocol, while investigating recombinant viruses tagged with a GFP protein [93]. Potentially, this effect can lose it importance over time after the absorption capacities are saturated by serum proteins of the culture medium. For the establishment of the extended infectivity assay in-house produced impedance sensors were used which also varied in their sensitivity. Standardization of such sensor most likely also would increase the robustness of the assay. Further, parameters such as fluid flow rate, culture chamber dimensions to further exploit flow dynamics or the seeding density of the indicator cell line are potential points for investigation for additional improvement of the assay.
Furthermore, the assay allows downstream analysis of the supernatant containing the virus with the purpose of determination of viral titres of unknown samples. Initially, MIP-QCM measurements were planned to be introduced downstream the extended impedance-based infectivity assay. However, due to initial difficulties in the establishment of viral imprints the establishment of the method at this time-point was postponed.

9 Bibliography

[1] E. J. Lefkowitz, D. M. Dempsey, R. C. Hendrickson, R. J. Orton, S. G. Siddell, and D. B. Smith, "Virus taxonomy: The database of the International Committee on Taxonomy of Viruses (ICTV)," *Nucleic Acids Res.*, vol. 46, no. D1, pp. D708–D717, 2018.

[2] P. P. Pastoret, "Human and animal vaccine contaminations," *Biologicals*, vol. 38, no. 3, pp. 332–334, 2010.

[3] M. T. Madigan and J. M. Martinko, "Essentials of Virology," in *Biology of Microorganisms*, 11th ed., Brock, 2006, pp. 230–255.

[4] T. Albrecht, M. Fons, I. Boldogh, and A. S. Rabson, "Effects on Cells," in *Medical Microbiology*, 4th ed., B. S, Ed. 1996.

[5] "The Vaccination History of Small-Pox Cases," *Br. Med. J.*, vol. 2, no. 2166, pp. 67–68, Jul. 1902.

[6] E. Ylösmäki and V. Cerullo, "Design and application of oncolytic viruses for cancer immunotherapy," *Curr. Opin. Biotechnol.*, vol. 65, no. Ici, pp. 25–36, 2020.

[7] N. Slade, "Viral vectors in gene therapy," *Period. Biol.*, vol. 103, no. 2, pp. 139–143, 2001.

[8] D. M. Lin, B. Koskella, and H. C. Lin, "Phage therapy: An alternative to antibiotics in the age of multi-drug resistance," *World J. Gastrointest. Pharmacol. Ther.*, vol. 8, no. 3, p. 162, 2017.

[9] C. Buttimer, O. McAuliffe, R. P. Ross, C. Hill, J. O'Mahony, and A. Coffey, "Bacteriophages and bacterial plant diseases," *Front. Microbiol.*, vol. 8, no. JAN, pp. 1–15, 2017.

[10] A. Baer and K. Kehn-Hall, "Viral concentration determination through plaque assays: Using traditional and novel overlay systems," *J. Vis. Exp.*, no. 93, pp. 1–10, 2014.

[11] M. J. Chiang, M. Pagkaliwangan, S. Lute, G. Bolton, K. Brorson, and M. Schofield, "Validation and optimization of viral clearance in a downstream continuous chromatography setting," *Biotechnol. Bioeng.*, vol. 116, no. 9, pp. 2292–2302, 2019.

[12] C. Stocking and C. A. Kozak, "Endogenous retroviruses: Murine endogenous retroviruses," *Cell. Mol. Life Sci.*, vol. 65, no. 21, pp. 3383–3398, 2008.

[13] A. A. Shukla and H. Aranha, "Viral clearance for biopharmaceutical downstream processes," *Pharm. Bioprocess.*, vol. 3, no. 2, pp. 127–138, 2015.

[14] FDA (Food and Drug Administration), "Testing of Retroviral Vector-Based Human Gene Therapy Products for Replication Competent Retrovirus During Product Manufacture and Patient Follow-Up - Draft Guidance for Industry," *Fda*, no. January, p. 16, 2020.

[15] A. Rein, "Murine leukemia viruses: Objects and organisms," *Adv. Virol.*, vol. 2011, 2011.

[16] J. W. Hartley, N. K. Wolford, L. J. Old, and W. P. Rowe, "A new class of murine leukemia virus A new class of murine leukemia virus associated with development of spontaneous lymphomas.," *Proc. Natl. Acad. Sci. U. S.*

A., vol. 74, no. 2, pp. 789–92, 1977.
[17] P. T. Peebles, "An in vitro focus-induction assay for xenotropic murine leukemia virus, feline leukemia virus C, and the feline-primate viruses RD-114/CCC/M-7," *Virology*, vol. 67, no. 1, pp. 288–291, 1975.
[18] D. K. Haapala, W. G. Robey, S. D. Oroszlan, and W. P. Tsai, "Isolation from cats of an endogenous type C virus with a novel envelope glycoprotein.," *J. Virol.*, vol. 53, no. 3, pp. 827–833, 1985.
[19] R. H. Bassin, S. Ruscetti, I. Ali, D. K. Haapala, and A. Rein, "Normal DBA/2 mouse cells synthesize a glycoprotein which interferes with MCF virus infection," *Virology*, vol. 123, no. 1, pp. 139–151, 1982.
[20] Z. Li, M. Blair, and L. Thorner, "PG-4 cell plaque assay for xenotropic murine leukemia virus," *J. Virol. Methods*, vol. 81, no. 1–2, pp. 47–53, 1999.
[21] M. Purtscher, M. Rothbauer, S. R. A. Kratz, A. Bailey, P. Lieberzeit, and P. Ertl, "A microfluidic impedance-based extended infectivity assay: combining retroviral amplification and cytopathic effect monitoring on a single lab-on-a-chip platform," *Lab Chip*, vol. 21, no. 7, pp. 1364–1372, 2021.
[22] J. M. Coffin, S. H. Hughes, and H. E. Varmus, "Purification, Composition, and Morphology of Virions," in *Retroviruses*, 1997.
[23] S. A. Aaronson and W. P. Rowe, "Nonproducer Clones of Murine BALB / 3T3 Sarcoma Transformed The study of viruses of the murine tumor complex has been advanced by the develop- ment of quantitative assays in tissue culture for murine sarcoma virus (MSV) (Hartley and Rowe , 1966) and m," *Virology*, vol. 42, pp. 9–19, 1970.
[24] S. A. Aaronson, R. H. Bassin, and C. Weaver, "Comparison of Murine Sarcoma Viruses in Nonproducer and S+L−-Transformed Cells," *J. Virol.*, vol. 9, no. 4, pp. 701–704, 1972.
[25] I. Giaever and C. R. Keese, "A morphological biosensor for mammalian cells," *Nature*, vol. 366, no. 6455, pp. 591–592, 1993.
[26] W. Gu and Y. Zhao, "Cellular electrical impedance spectroscopy: An emerging technology of microscale biosensors," *Expert Rev. Med. Devices*, vol. 7, no. 6, pp. 767–779, 2010.
[27] H. S. Lew and Y. C. Fung, "On the low-Reynolds-number entry flow into a circular cylindrical tube.," *J. Biomech.*, vol. 2, no. 1, pp. 105–119, Mar. 1969.
[28] P. Abgrall and A. M. Gué, "Lab-on-chip technologies: Making a microfluidic network and coupling it into a complete microsystem - A review," *J. Micromechanics Microengineering*, vol. 17, no. 5, 2007.
[29] J. Ducrée and R. Zengerle, *FlowMap: Microfluidics Roadmap for the Life Sciences*. 2004.
[30] P. Novo, M. Dell'Aica, D. Janasek, and R. P. Zahedi, "High spatial and temporal resolution cell manipulation techniques in microchannels," *Analyst*, vol. 141, no. 6, pp. 1888–1905, 2016.
[31] P. Cui and S. Wang, "Application of microfluidic chip technology in pharmaceutical analysis: A review," *J. Pharm. Anal.*, vol. 9, no. 4, pp. 238–247, 2019.
[32] Chiu JJ, "NIH Public Access," *Physiol rev*, vol. 91, no. 1, pp. 1–106, 2011.
[33] J. M. Rutkowski and M. A. Swartz, "A driving force for change: interstitial flow as a morphoregulator," *Trends Cell Biol.*, vol. 17, no. 1, pp. 44–50, 2007.

[34] N. Azizipour, R. Avazpour, D. H. Rosenzweig, M. Sawan, and A. Ajji, "Evolution of biochip technology: A review from lab-on-a-chip to organ-on-a-chip," *Micromachines*, vol. 11, no. 6, pp. 1–15, 2020.
[35] A. R. Wu and L. Yu, "There's plenty of room at the bottom of a cell," *Chem. Eng. Prog.*, vol. 113, no. 10, 2017.
[36] T. J. Clark, P. H. McPherson, and K. F. Buechler, "The Triage Cardiac Panel," *Point Care J. Near-Patient Test. Technol.*, vol. 1, no. 1, pp. 42–46, 2002.
[37] M. I. Mohammed, S. Haswell, and I. Gibson, "Lab-on-a-chip or Chip-in-a-lab: Challenges of Commercialization Lost in Translation," *Procedia Technol.*, vol. 20, no. July, pp. 54–59, 2015.
[38] A. Hasan *et al.*, "Recent advances in application of biosensors in tissue engineering," *Biomed Res. Int.*, vol. 2014, 2014.
[39] Y. Ye, H. Guo, and X. Sun, "Recent progress on cell-based biosensors for analysis of food safety and quality control," *Biosens. Bioelectron.*, vol. 126, pp. 389–404, 2019.
[40] P. Banerjee and A. K. Bhunia, "Mammalian cell-based biosensors for pathogens and toxins," *Trends Biotechnol.*, vol. 27, no. 3, pp. 179–188, 2009.
[41] T. Chalklen, Q. Jing, and S. Kar-Narayan, "Biosensors based on mechanical and electrical detection techniques," *Sensors (Switzerland)*, vol. 20, no. 19, pp. 26–37, 2020.
[42] G. Evtugyn, *Biosensors : Essentials*, vol. 84. 2014.
[43] H. T. Ngoc Le, J. Kim, J. Park, and S. Cho, "A Review of Electrical Impedance Characterization of Cells for Label-Free and Real-Time Assays," *Biochip J.*, vol. 13, no. 4, pp. 295–305, 2019.
[44] B. Srinivasan, A. R. Kolli, M. B. Esch, H. E. Abaci, M. L. Shuler, and J. J. Hickman, "TEER Measurement Techniques for In Vitro Barrier Model Systems," *J. Lab. Autom.*, vol. 20, no. 2, pp. 107–126, 2015.
[45] L. Shuler and J. J. Hickman, *TEER measurement techniques for in vitro barrier model systems*, vol. 20, no. 2. 2016.
[46] "PNAS-1984-Giaever-3761-4.pdf." .
[47] S. Rahim and A. Üren, "A Real-time Electrical Impedance Based Technique to Measure Invasion of Endothelial Cell Monolayer by Cancer Cells," no. Figure 2, pp. 10–13, 2011.
[48] J. Wegener, C. R. Keese, and I. Giaever, "Electric Cell – Substrate Impedance Sensing (ECIS) as a Noninvasive Means to Monitor the Kinetics of Cell Spreading to Artificial Surfaces," vol. 166, pp. 158–166, 2000.
[49] Y. Koo and Y. Yun, "Effects of polydeoxyribonucleotides (PDRN) on wound healing : Electric cell-substrate impedance sensing (ECIS)," *Mater. Sci. Eng. C*, vol. 69, pp. 554–560, 2016.
[50] M. Cobb, "60 years ago, Francis Crick changed the logic of biology," *PLoS Biol.*, vol. 15, no. 9, pp. 1–8, 2017.
[51] N. Grandi and E. Tramontano, "Human endogenous retroviruses are ancient acquired elements still shaping innate immune responses," *Front. Immunol.*, vol. 9, no. SEP, pp. 1–16, 2018.
[52] E. J. Grow *et al.*, "Intrinsic retroviral reactivation in human preimplantation embryos and pluripotent cells," *Nature*, vol. 522, no. 7555, pp. 221–246, 2015.
[53] A. Rodrigues, P. Alves M., and A. Coroadinh, "Production of Retroviral and

Lentiviral Gene Therapy Vectors: Challenges in the Manufacturing of Lipid Enveloped Virus," *Viral Gene Ther.*, 2011.
[54] N. J. MacLachlan, E. J. Dubovi, S. W. Barthold, D. E. Swayne, and J. R. Winton, "Fenner's Veterinary Virology," in *Fenner's Veterinary Virology*, 2017, pp. 269–297.
[55] E. Hunter, "Viral Entry and Receptors," in *Retroviruses*, Cold Spring Harbor (NY), 1997.
[56] J. Coffin, S. Hughes, and H. Varmus, "Overview of Reverse Transcription," in *Retroviruses*, Cold Spring Harbor (NY), 1997.
[57] H. Fan and D. Baltimore, "RNA metabolism of murine leukemia virus: Detection of virus-specific RNA sequences in infected and uninfected cells and identification of virus-specific messenger RNA," *J. Mol. Biol.*, vol. 80, no. 1, pp. 93–117, 1973.
[58] J. Coffin, S. Hughes, and H. Varmus, "Processing of Retroviral RNA," in *Retroviruses*, 1997.
[59] A. Shields, W. N. Witte, E. Rothenberg, and D. Baltimore, "High frequency of aberrant expression of Moloney murine leukemia virus in clonal infections.," *Cell*, vol. 14, no. 3, pp. 601–9, 1978.
[60] S. Cen *et al.*, "Retrovirus-specific packaging of aminoacyl-tRNA synthetases with cognate primer tRNAs.," *J. Virol.*, vol. 76, no. 24, pp. 13111–5, 2002.
[61] J. Konvalinka, H. G. Kräusslich, and B. Müller, "Retroviral proteases and their roles in virion maturation," *Virology*, vol. 479–480, pp. 403–417, 2015.
[62] C. J. Tabin, J. W. Hoffmann, S. P. Goff, and R. A. Weinberg, "Adaptation of a retrovirus as a eucaryotic vector transmitting the herpes simplex virus thymidine kinase gene.," *Mol. Cell. Biol.*, vol. 2, no. 4, pp. 426–36, 1982.
[63] W. S. Hu and V. K. Pathak, "Design of retroviral vectors and helper cells for gene therapy.," *Pharmacol. Rev.*, vol. 52, no. 4, pp. 493–511, 2000.
[64] L. M. Muul *et al.*, "Persistence and expression of the adenosine deaminase gene for 12 years and immune reaction to gene transfer components: Long-term results of the first clinical gene therapy trial," *Blood*, vol. 101, no. 7, pp. 2563–2569, 2003.
[65] M. A. Morgan, M. Galla, M. Grez, B. Fehse, and A. Schambach, "Retroviral gene therapy in Germany with a view on previous experience and future perspectives," *Gene Ther.*, 2021.
[66] V. C. Emery, "Production of plaques in monolayer tissue cultures by single particles of an animal virus," *Rev. Med. Virol.*, vol. 6, no. 2, pp. 61–64, 1996.
[67] L. J. R. H. Muench, "A Simple Method of Estimating Fifty Percent Endpoints," *Am. J. Hygine*, vol. 27, pp. 493–497, 1938.
[68] A. F. Payne, I. Binduga-Gajewska, E. B. Kauffman, and L. D. Kramer, "Quantitation of flaviviruses by fluorescent focus assay," *J. Virol. Methods*, vol. 134, no. 1–2, pp. 183–189, 2006.
[69] G. K. Hirst, "The Quantitative Determination of Influenza Virus and Antibodies by Means of Red Cell Aggluatination" *J. Exp. Med.*, pp. 49–64, 1942.
[70] P. K. Smith *et al.*, "Measurement of protein using bicinchoninic acid," *Anal. Biochem.*, vol. 150, no. 1, pp. 76–85, 1985.
[71] H. Pyra, J. Böni, and J. Schüpbach, "Ultrasensitive retrovirus detection by a reverse transcriptase assay based on product enhancement," *Proc. Natl.*

Acad. Sci. U. S. A., vol. 91, no. 4, pp. 1544–1548, 1994.
[72] M. A. Liebert *et al.*, "Replication-Competent Retrovirus and Lentivirus Detection," vol. 1236, no. October, pp. 1227–1236, 2005.
[73] A. Malmsten *et al.*, "A colorimetric reverse transcriptase assay optimized for Moloney murine leukemia virus, and its use for characterization of reverse transcriptases of unknown identity," *J. Virol. Methods*, vol. 75, no. 1, pp. 9–20, 1998.
[74] M. Hercher, W. Mueller, and H. M. Shapiro, "Detection and Discrimination of Individual Viruses by Flow Cytometry," *J. Histochem. Cytochem. J. Histochem. Cytochem.*, vol. 27, pp. 350–352, 1979.
[75] M. Gao *et al.*, "Recent Advances and Future Trends in the Detection of Contaminants by Molecularly Imprinted Polymers in Food Samples," *Front. Chem.*, vol. 8, no. December, pp. 1–20, 2020.
[76] M. Hussain, K. Kotova, and P. A. Lieberzeit, "Molecularly imprinted polymer nanoparticles for formaldehyde sensing with QCM," *Sensors (Switzerland)*, vol. 16, no. 7, 2016.
[77] M. Jenik, A. Seifner, P. Lieberzeit, and F. L. Dickert, "Pollen-imprinted polyurethanes for QCM allergen sensors," *Anal. Bioanal. Chem.*, vol. 394, no. 2, pp. 523–528, 2009.
[78] Z. Pei, J. Saint-Guirons, C. Käck, B. Ingemarsson, and T. Aastrup, "Real-time analysis of the carbohydrates on cell surfaces using a QCM biosensor: A lectin-based approach," *Biosens. Bioelectron.*, vol. 35, no. 1, pp. 200–205, 2012.
[79] Z. Farka, D. Kovář, and P. Skládal, "Rapid detection of microorganisms based on active and passive modes of QCM," *Sensors (Switzerland)*, vol. 15, no. 1, pp. 79–92, 2015.
[80] M. R. Lander and S. K. Chattopadhyay, "A Mus dunni Cell Line That Lacks Sequences Closely Related to Endogenous Murine Leukemia Viruses and Can Be Infected by Ecotropic, Amphotropic, Xenotropic, and Mink Cell Focus-Forming Viruses," *J. Virol.*, vol. 52, no. 2, pp. 695–698, 1984.
[81] D. K. Haapala, W. G. Robey, S. D. Oroszlan, and W. P. Tsai, "Isolation from cats of an endogenous type C virus with a novel envelope glycoprotein.," *J. Virol.*, vol. 53, no. 3, pp. 827–833, 1985.
[82] J. A. Levy *et al.*, "Murine xenotropic type C viruses. IV. Replication and pathogenesis in ducks," *J. Gen. Virol.*, vol. 61, no. 1, pp. 65–74, 1982.
[83] M. Purtscher, M. Rothbauer, S. R. A. Kratz, A. Bailey, P. Lieberzeit, and P. Ertl, "Supporting information: A microfluidic impedance-based extended infectivity assay: Combining retroviral amplification and cytopathic effects monitoring on a single lab-on-a-chip platform," *Lab Chip*, vol. 21, no. 7, 2021.
[84] S. Lebourgeois, A. Fraisse, C. Hennechart-Collette, L. Guillier, S. Perelle, and S. Martin-Latil, "Development of a Real-Time Cell Analysis (RTCA) Method as a Fast and Accurate Method for Detecting Infectious Particles of the Adapted Strain of Hepatitis A Virus," *Front. Cell. Infect. Microbiol.*, vol. 8, no. September, p. 335, 2018.
[85] M. R. Pennington and G. R. Van de Walle, "Electric Cell-Substrate Impedance Sensing To Monitor Viral Growth and Study Cellular Responses to Infection with Alphaherpesviruses in Real Time," *mSphere*, vol. 2, no. 2, pp. 1–12, 2017.

[86] Y. Zhu, J. W. Warrick, K. Haubert, D. J. Beebe, and J. Yin, "Infection on a chip: A microscale platform for simple and sensitive cell-based virus assays," *Biomed. Microdevices*, vol. 11, no. 3, pp. 565–570, 2009.
[87] E. Cimetta *et al.*, "Microfluidic-driven viral infection on cell cultures: Theoretical and experimental study," *Biomicrofluidics*, vol. 6, no. 2, pp. 1–12, 2012.
[88] B. Alberts, A. Johnson, J. Lewis, M. Raff, K. Roberts, and P. Walter, "The Cell Cycle," in *Molecular Biology of The Cell*, 2008, pp. 1053–1204.
[89] S. T. Andreadis, D. Brott, and A. O. Fuller, "Moloney Murine Leukemia Virus-Derived Retroviral Vectors Decay Intracellularly with a Half-Life in the Range of 5 . 5 to 7 . 5 Hours," vol. 71, no. 10, pp. 7541–7548, 1997.
[90] S. Andreadis and B. O. Palsson, "Kinetics of Retrovirus Mediated Gene Transfer : The Importance of Intracellular Half-Life of Retroviruses," pp. 1–20, 1996.
[91] J. Campisi and E. E. Medrano, "Cell cycle perturbations in normal and transformed fibroblasts caused by detachment from the substratum," *J. Cell. Physiol.*, vol. 114, no. 1, pp. 53–60, 1983.
[92] C. Charretier *et al.*, "Robust real-time cell analysis method for determining viral infectious titers during development of a viral vaccine production process," *J. Virol. Methods*, vol. 252, no. April 2017, pp. 57–64, 2018.
[93] N. Xu *et al.*, "A microfluidic platform for real-time and in situ monitoring of virus infection process," *Biomicrofluidics*, vol. 6, no. 3, pp. 1–9, 2012.

10 List of Equations

11 List of Figures

12 List of Abbreviations

Abbreviation	Long name	Short description (as used in this work)
AC	Alternating current	alternating electrical current, periodically reversing direction
BCA	Bicinchoninic acid assay	assay to determine protein
BrdUTP	5-bromo-deoxyuridine-57-triphosphate	synthetic analogue for thymidine
CA	Capsid	viral capsid protein
CPE	Cytopathic effects	structural changes in virus infected cells
DC	Direct current	one directional electrical current,
ECIS	Electrical cell-substrate impedance sensing	measurement of changes in cellular layer by means of impedance spectroscopy
EIS	Electrical impedance spectroscopy	measurement of the resistance over a range of frequencies
ELISA	Enzyme-linked immunosorbent assay	antibody detection-based biochemistry assay

EVOM™	Epiethelial Voltohmmeter	Device to measure TEER values over cell layer
FACS	Fluorescence-activated cell sorting	determination of cell populations based on specific fluorescence labelling of the cells
FCS	Foetal calf serum	cell culture ingredient
FFA	Fluorescence focus assay	Fluorescence based viral detection method
HA	Hemagglutination assay	Viral detection assay method based on red blood cell coagulation
HAU	Hemagglutination units	Units to describe virus load of hemagglutination assay
ICTV	International Committee on Taxonomy of Viruses	
IN	Integrase	Retroviral enzyme necessary for the viral genome to integrate into the host cell
LOC	Lab-on-Chip	Device with more than one laboratory functions or working steps combined
LTR	Long Term Repeats	Viral genome structure necessary to integrate into the hosts genome
MA	Matrix protein	Protein compound of the viral structure
MEMS	micro-electro-mechanical systems	Technology integrating electrical and mechanical parts on a nanometre scale
MIP	Molecular imprinted polymers	Polymers selective to ligands based on structural and conformational attributes
MuLV	Murine leukemia virus	Retrovirus model system
MOI	Multiplicity of infection	Numbers of virions added per cell
NC	Nucleocapsid protein	Protein compound of the viral capsid structure
PBS	Primer binding site	Sequence for polymerase attachment and signal for synthetization start
PDMS	Polydimethylsiloxane	Polymer used to build fluidic layers
PFU	Plaque forming unit	Unit to determine viral titre
PPT	Polypurine tract	Sequence on the viral genome necessary for the reverse transcriptase process
PR	Protease	Enzyme necessary to breakdown proteins

QCM	Quartz crystal microbalance	Highly sensitive method to measure changes in masses
qPCR	Quantitative polymerase chain reaction	Method to measure DNA content based on increasing fluorescence signal during amplification of those molecules
R	Direct repeats	Viral genome structure necessary to integrate into the hosts genome
RT	Reverse transcriptase	Enzyme catalysing the transcription of the viral RNA into DNA
SU	Surface protein	Protein compound of the viral structure
TCID50	Median culture infection dose	Number of virus particle which will have CPEs on 50 % of the cell culture
TEER	Transepithelial electrical resistance	Measurement of the resistance of a cellular barrier
TM	Transmembrane protein	Protein compound of the viral structure
U3	Unique regulatory sequences at the 3' end	Regulatory unit of the viral genome
U5	Unique regulatory sequences the 5' end	Regulatory unit of the viral genome
x-MuLV	Xenotropic murine leukemia virus	Retrovirus inducing leukemia in mice and other rodents
PCR	Polymerase chain reaction	Method to amplify DNA sequences
µTAS	micro-total-analysis systems	System which integrates all steps of an assay to detect an analyte on a microscale device